The 21st Workshop on Antarctic Meteorology and Climate

Charleston, SC, USA

16-18 June 2026

Sponsored by the National Science Foundation

On behalf of the Planning Committee, we welcome you to Charleston, South Carolina for the 21st Workshop on Antarctic Meteorology and Climate (WAMC). This meeting brings together those with common interests in Antarctic meteorology, climate, forecasting and related disciplines to discuss the myriad issues that each of us face: from numerical modeling, observational systems, and forecasting challenges. This year we have dedicated a session to discussions on the technology behind surface and other environmental sensing systems critical to understanding more about the Antarctic. We hope that this will serve as a valuable forum for you to share your current results and ideas and to learn from this unique community.

The history of this workshop dates back nearly 50 years through differing meetings, with early gatherings on the automatic weather station programs in the 1980s to discussions focused on numerical weather prediction systems. The first iteration of this workshop served to unite these various topics in Antarctic meteorology into an active and centralized forum for efficient and effective efforts in pursuit of science. We hope to continue this tradition through robust dialog on the successes and challenges facing the various facets of Antarctic meteorology and further improving our understanding of this mystifying environment.

We thank each one who has submitted abstracts and presentations as well as each attendee. We look forward to healthy discussion and discovery throughout this week, and that everyone will find these sessions to be informative and productive.

Special recognition is due to the Chickasaw Alliance Group team of Jacki Major, Star Fluerty, Fred Garcia, and Joey Snarski, for their incredible efforts in coordinating the logistical needs of this workshop. We would also be remiss if we didn't thank Matt Lazzara, Taylor Ziegler, Sophie Orendorf, and Mary Reinhardt from the University of Wisconsin-Madison for their help in advertising and managing the digital footprint necessary for this event. Finally, we'd like to thank the volunteer session chairs and student assistants from the College of Charleston.

The 21st WAMC is organized by the Naval Information Warfare Center Atlantic Polar Programs team and is sponsored by the National Science Foundation Office of Polar Programs. Again, we thank you for your participation, ask you to be careful in the heat, and hope you enjoy your time here in the Lowcountry.

Local Organizing Committee:
Michael Johnson, Chair
Bella Onsi
Paul Gulli
Jenna Palmer
Shane Thornton

21ST WORKSHOP ON ANTARCTIC METEOROLOGY AND CLIMATE
HILTON GARDEN INN CHARLESTON WATERFRONT/DOWNTOWN
45 LOCKWOOD DRIVE, CHARLESTON, SC
JUNE 16 – 18 2026

Monday, 15 June 2026

1800-2000	Informal Icebreaker 45 Waterside at the Hilton Garden Inn (In case of inclement weather: Peninsula Pre-Function)

Tuesday, 16 June 2026

0830-0900	Registration Peninsula Pre-Function
0900-0920	Opening Remarks and Information Bruce Carter, NIWC LANT Shore C2ISR and Integration Department Head
0920-0940	Our Antarctic Community / Personal Introductions Michael Johnson, NIWC LANT Polar Programs
Session 1:	**Policy and Operations** **Chair: Bella Onsi, NIWC LANT Polar Programs**
0940-1000	An update on the activities of the WMO's Antarctic Advisory Group and GCW (Virtual) Steve Colwell
1000-1020	Break Peninsula Pre-Function
1020-1040	Climatological Support and Data Acquisition in the Antarctic: Operations of the 14th Weather Squadron Jason Patla, David Kofron, and Samat Siwek
1040-1100	NPP Meteorology 2026: Overview, Plans, and Goals Michael Johnson
1100-1120	Forecast Watches, Warnings and Advisories for McMurdo Station and its Airfields Paul Gulli
1120-1300	Lunch

Session 2: **Observations and Data**
Chair: Brian Rakoczy, The Ohio State University

1300-1320 Automatic Weather Station field season review 2025-26
Lee Welhouse

1320-1340 An Overview of AWS Servicing at Halley and Rothera Research Stations During the 2025/26 Season (Recorded)
Sabina Kucieba, Steve Colwell, and Alice Clement

1340-1400 The Madison Automatic Weather Station: Next-Generation Development and Operational Successes
Forbes A. Filip

1400-1420 NPP Meteorological Systems
Matt Frazier and Bella Onsi

1420-1440 Break
Peninsula Pre-Function

1440-1500 Quality Control Procedures for an Antarctic Automatic Weather Station Network (Virtual)
Sophie Orendorf, Taylor Ziegler, David Mikolajczyk, Linda Keller, and Matthew Lazzara

1500-1520 Observational Data Availability at South Pole Station and Impact on Forecasting Operations
Jenna Palmer

1520-1540 Portable Doppler Radar (PDR) Project
Ragen Willaford-Menefee

1540-1600 AMRDC Observational Data Update (Virtual)
David Mikolajczyk, Matthew Lazzara, Caleb Cullum, Sophie Orendorf, Taylor Ziegler, Lee Welhouse, and Karissa Shannon

1600-1620 Polar Potpourri: Status and the Near-Future of AWS and AMRDC projects
Matthew A. Lazzara, Andy Kurth, Forbes Filip, David Mikolajczyk, Matthew Noojin, Sophie Orendorf, Karissa Shannon, Lee Welhouse, and Taylor Ziegler

1620-1630 End-of-Day Remarks

Wednesday, 17 June 2026

0830-0900 Registration
Peninsula Pre-Function

Session 3A: Numerical Modeling (AM)
Chair: Jenna Palmer, NPP / CAG

0900-0920 AMPS Update -- June 2026
Kevin W. Manning and Jordan G. Powers

0920-0940 Performance of Polar WRF in the Polar Regions and Transition to a Regional Earth System Model
David H. Bromwich, Lesheng Bai, Keith M. Hines, Saurav dey Shuvo, and Rui Sun

0940-1000 A Polar WRF and Unified Model Study of an Atmospheric River Event at Davis, Antarctica
Keith M. Hines, Sonya Fiddes, Simon Alexander, David H. Bromwich, Mariana Fontolan Litell, Sheng-Hung Wang, and Zhangcheng Pei

1000-1020 Break
Peninsula Pre-Function

1020-1040 Evaluation of AI-Based Weather Forecasts over the Southern Polar Region
Brian Rakoczy, Saurav Dey Shuvo, David Bromwich, Sheng-Hung Wang

1040-1100 Characterization of Drifting and Blowing Snow at PEA Station and Validation of the CRYOWRF Model (Virtual)
Lorena Accossato, Rainette Engbers, and Michael Lehning

1100-1120 Antarctic Winter Numerical Forecast Improvement from Enhanced… Radiosondes (YOPP-SH)
Mariana Fontolan Litell, David H. Bromwich, Jordan G. Powers, Kevin W. Manning, and Sheng-Hung Wang

1120-1300 Lunch
(WAMC Planning Committee Meeting)

Session 3B: Numerical Modeling (PM)
Chair: Mariana Fontolan Litell, The Ohio State University

1340-1400 MPAS-A Performance in the Polar Regions
David H. Bromwich, Lesheng Bai, and Qian Xu

1400-1420 Drivers of observed winter–spring sea-ice and snow thickness at a coastal site in East Antarctica (Virtual)
Ricardo Fonseca, Diana Francis, Narendra Nelli, Petra Heil; Jonathan Wille, Irina Gorodetskaya, and Robert Massom

1420-1440 Break
Peninsula Pre-Function

1440-1500 Contrasting Radiative Regimes in Antarctica: Empirical and ARDL Modeling and Attribution of Global Solar Radiation Losses at Dome C and Horseshoe Island (Virtual)
Erhan Arslan

1500-1520 Analysis of an Antarctic Atmospheric Mass Loss Event (MPAS)
Jordan Powers

1520-1540 March 2022 East Antarctic heatwave under different background climate conditions (Model simulations)
Xun Zou, Edward Blanchard-Wrigglesworth, Zhenhai Zhang, Matthew R. Mazloff, Benjamin Moore, Dan Lubin, Matthew A. Lazzara, Irina V. Gorodetskaya, Jason M. Cordeira, Matthew Simpson, Brian Kawzenuk, Jinxi Li, Lanhao Yang, Penny M. Rowe, and F. Martin Ralph

1540-1600 Presentation: Polar Coupled Analysis and Prediction for Services (PCAPS) (Virtual)
Daniela Liggett

Special Discussion:

1600-1620 Discussion: Operational Meteorology Coordination
Michael Johnson & Paul Gulli

1620-1630 End-of-Day Remarks

Thursday, 18 June 2026

0830-0900 Registration
Peninsula Pre-Function

Session 4: Forecasting and Climatic Studies
Chair: Regan Willaford-Menefee, NIWC LANT Polar Programs

0900-0920 A 30-Year Satellite Derived Climatology of Landfalling Antarctic Cloud Mass Meridional Transport Events (Virtual)
Jonathan Chambers, Matthew Lazzara, Hannah Zanowski, David Mikolajczyk, Caleb Cullum, and Mary Reinhardt

0920-0940 Heatwaves in the East Antarctic interior amplified by climate change (Virtual)
Naoyuki Kurita, David H. Bromwich, and Matthew A. Lazzara

0940-1000 How much do extreme snow events contribute to the mass of the Antarctic Ice Sheet? (Virtual)
Karissa Shannon, Tristan L'Ecuyer, and Marian Mateling

1000-1020 Break
Peninsula Pre-Function

1020-1040	Revisiting the extraordinary katabatic wind regime at Terra Nova Bay, Antarctica Brian Rakoczy, David Bromwich, Matthew Lazzara, and Paolo Grigioni
1040-1100	A November Snow Event at McMurdo Station (Radar Justification) John R. Michael
1100-1120	Use of Tall Tower Data in Operational Forecasting Bella Onsi
1120-1300	Lunch
Session 5:	**Technology Discussions and Conclusion** **Chair: Michael Johnson, NIWC LANT Polar Programs**
1300-1600	Discussion: Meteorological Observations and Data: A Workshop Discussion Matthew A. Lazzara
	Discussion: AWS Technology
	Discussion: DBRS Technology
1600-1630	End of Meeting Remarks, Announcements, and Action Items Michael Johnson

AN UPDATE ON THE ACTIVITIES OF THE WORLD METEOROLOGICAL SOCIETY'S ANTARCTIC ADVISORY GROUP AND GLOBAL CRYOSPHERE WATCH ACTIVITIES

Steve Colwell
British Antarctic Survey

I will present an update on the activities of the World Meteorological Society's Antarctic Advisory Group including the first Antarctic Climate Forum meeting hosted at BAS in January 2026. I will also give an update from the Global Cryosphere Watch steering committee meeting held in Geneva from the 8th-12th June and highlight items that are relevant to the Antarctic community.

CLIMATOLOGICAL SUPPORT AND DATA ACQUISITION IN THE ANTARCTIC: OPERATIONS OF THE 14TH WEATHER SQUADRON

Jason Patla, David Kofron, Samat Siwek
14th Weather Squadron

The 14th Weather Squadron (14 WS) provides key climatological support to the USAP and related military support organizations through the Support Assistance Request process. This presentation outlines the operational capabilities and data challenges faced by the 14 WS in the Antarctic region. While the 14 WS maintains a robust global dataset of meteorological and hydrological observations, significant data gaps persist in Antarctica. Large areas of the continent remain unobserved, and many existing locations only provide seasonal data. Consequently, there is an ongoing operational imperative to acquire comprehensive meteorological data across the region to close these gaps. Despite observation limitations, the 14 WS actively leverages its existing database to deliver a wide range of tailored meteorological products to the USAP. This support spans standard surface climatology, flight-level winds, wind roses, and ceiling and visibility assessments. As the squadron's database across and around Antarctica continues to grow and improve, its ability to effectively support diverse and complex mission sets in this extreme environment will correspondingly increase. This briefing will highlight current data acquisition needs, operational support capabilities, and the direct impact of expanded data collection on USAP mission success.

NPP METEOROLOGY 2026: OVERVIEW, PLANS, AND GOALS

Michael D. Johnson
NIWC LANT Polar Programs

This presentation will provide a summary of NPP Meteorology activities over the past Austral Summer season and future goals for the next Austral Summer season and beyond. In the 2025-26 season, NPP Meteorology returned to a historical staffing arrangement, with forecasting services evenly split between our Remote Operating Facility in North Charleston, SC and McMurdo Station, with continued airfield and upper air observations. Near continuous aviation weather observations were provided from Phoenix Airfield for much of the season, relaxing some logistical constraints for airlift operations. For the 2026-27 season, new constraints are expected to force some changes in how services are provided, with increased automation, as well continued efforts to enhance integration of weather data into program planning. Capital acquisition projects for a weather radar and updated satellite data acquisition system are progressing, along with smaller system improvements to existing programs.

FORECAST WATCHES, WARNINGS AND ADVISORIES FOR MCMURDO STATION AND ITS AIRFIELDS

Paul Gulli
NPP/CAG

While an effective tool for communicating adverse weather, the current Severe Weather Conditions system only addresses observed criteria. Forecasters have traditionally communicated expected conditions through the McMurdo Daily forecast and airfield TAFs but must wait for these conditions to be observed before issuing warnings to the community. Additionally, the criteria for the SWC product begin below most aviation thresholds, thereby not being as useful to aviators as they are to other entities such as cargo, refuelers or fleet operators. To address this, NPP Meteorology is developing a forecast Watch, Warning and Advisory product to provide a more robust, tailored advance notice of expected weather impacts.

AUTOMATIC WEATHER STATION FIELD SEASON REVIEW 2025-26

Lee Welhouse
Antarctic Meteorological Research and Data Center

The 2025-26 field season had 4 primary goals for the Automatic Weather Station program. Install a new system at Cape Hallett, install a radiation shield evaluation system at South Pole Station, service the highest priority systems in West Antarctica, and continue maintenance on the remaining systems possible out of McMurdo. To do the work we planned to deploy two teams, the first consisting of Lee Welhouse and Matthew Lazzara and the second consisting of Forbes Filip. Due to unforeseen complications and weather issues both Cape Hallett and South Pole systems could not be installed. Fortunately, significantly more success was achieved in the maintenance of systems in West Antarctica, and the continued maintenance of systems from McMurdo station. We will review the full field season and strategies for dealing with the new challenges as they arise.

AN OVERVIEW OF AWS SERVICING AT HALLEY AND ROTHERA RESEARCH STATIONS DURING THE 2025/26 SEASON

Sabina Kucieba, Steve Colwell, Alice Clement
British Antarctic Survey

Automatic Weather Stations (AWS) maintained by the British Antarctic Survey were visited in the Antarctic summer season. Initial inspection of the instruments, data collection, instruments raise, battery inspection and replacement, any necessary repairs, and data flow check after raise were performed on site. All sites were visited this year (7 BAS sites and 2 Non-BAS sites) and are prepared for the winter. A summary of all done work and any issues that arose on site will be presented. Data from these sites are essential, as they are transmitted via satellite to global meteorological centres and are used in weather forecasting models.

THE MADISON AUTOMATIC WEATHER STATION: NEXT-GENERATION DEVELOPMENT AND OPERATIONAL SUCCESSES

Forbes A. Filip
AMRDC

The Madison Automatic Weather Station (AWS) program continues development and modernization efforts focused on improving autonomous observing systems supporting atmospheric and meteorological research in Antarctica. This presentation will provide an overview of the state of the Madison AWS system following the 2025-2026 field season and efforts to improve observability, diagnostics, and field serviceability. Lessons learned from development, integration, and deployment efforts will also be discussed. Future plans for the Madison AWS system for the 2026-2027 field season and beyond include continued refinement of the hardware and software ecosystem, expanded instrumentation capabilities (e.g., radiometers, acoustic depth gauges), operational usability improvements, and further system improvements intended to support long-term scientific observations and operations.

NPP METEOROLOGICAL SYSTEMS

Matt Frazier, Bella Onsi
NPP/CAG

NPP’s ground electronics and maintenance team is tasked with servicing all airfield landing equipment at the McMurdo Station area airfields, as well as the upkeep of NPP’s own network of weather sensors on the ice including FMQs, automatic weather stations (AWS), and Wind Alert systems. This presentation will provide an overview of the maintenance completed on NPP's AWS and the FMQ at South Pole Station during the 2025-2026 operational season, along with goals for the following operational season.

QUALITY CONTROL PROCEDURES FOR AN ANTARCTIC AUTOMATIC WEATHER STATION NETWORK

Sophie Orendorf, Taylor Ziegler, David Mikolajczyk, Linda Keller, Matthew Lazzara
Antarctic Meteorological Research and Data Center

Data collection has long been a challenge in Antarctica due to the harsh environment and lack of staffed stations around the continent. Automatic weather stations (AWS) are utilized around the continent by numerous agencies, including the Antarctic Meteorological Research and Data Center (AMRDC), to fill in gaps in data collection. The AMRDC has the largest AWS network on the continent that produces quality controlled (QC) versions of their data to the public. Utilizing AWS presents complications due to limited site visits, lack of sensors, and engineering that can survive the austral winters. Ensuring data accuracy, especially in such a data-sparse region, leads to the ability to conduct better climatological analyses and ensure reliable study of extreme weather events. While most midlatitude weather stations distribute raw data and/or utilize automatic QC procedures, the AMRDC has a combination of manual and automatic QC processes. The procedure factors in the intricacies of the sensors, their relationship and behavior in Antarctica, and known limitations with the data collection. We will discuss our current QC process so that other research groups who wish to provide QC versions of their data to the scientific community can learn about our in depth procedure.

To accommodate the various and ever-expanding sensor suites across the AMRDC AWS network, a new QC application has been developed utilizing the Python programming language. AMRDC's current QC process is tedious and time consuming, and the current software is difficult to modify due to the lack of knowledge with the current personnel. The new application is tailored to the AMRDC, with a flexible framework that allows for maximum versatility for future needs. In addition, a special application was developed to quality control all observation levels of the two tall tower AWS that the AMRDC currently operates. The ability to QC historical data and tall tower data allows for further scientific studies utilizing AMRDC AWS data.

OBSERVATIONAL DATA AVAILABILITY AT SOUTH POLE STATION AND IMPACT ON FORECASTING OPERATIONS

Jenna Palmer
NPP/CAG

Flight operations at the South Pole depend on the quality of observation and forecasts, particularly present weather, ceilings, and visibility. Currently, the primary hindrance to insightful data analysis is the quality and frequency of incoming observations from the South Pole. Forecasters rely only on satellite imagery to gauge the timing of incoming weather; there are very limited live resources and no method of data validation during blackout periods or satellite outages. Therefore, data analysis on visibility forecasts is limited to reported METAR variables and readings from other surrounding sensors. The current landscape of available data archives significantly limits the applicable data analysis techniques on the current data sets. This project investigates the historical data on present weather and visibility and attempts to identify significant visibility trends with other surrounding sensors. Through data analysis of adjacent weather stations, it is possible to derive additional insights regarding visibility. With careful data cleaning and comparisons, some insights can be derived that may help improve visibility forecasts.

PORTABLE DOPPLER RADAR (PDR) PROJECT

Ragen Willaford-Menefee
NIWC LANT Polar Programs

NIWC Polar Programs (NPP) is dedicated to advancing meteorological operations and real-time forecasting in support of the United States Antarctic Program (USAP). To this end, NPP is implementing the National Science Foundation (NSF)-funded Portable Doppler Radar (PDR) project at McMurdo Station, Antarctica. This presentation outlines the project's operational requirements, estimated installation timeline, and anticipated mission benefits, while also addressing site-selection, and operational challenges.

Antarctic Meteorological Research and Data Center Observational Data Update

David Mikolajczyk[1], Matthew Lazzara[1,2], Caleb Cullum[1], Sophie Orendorf[1], Taylor Ziegler[1], Lee Welhouse[1], and Karissa Shannon[1]

[1]Antarctic Meteorological Research and Data Center, Space Science and Engineering Center, University of Wisconsin-Madison, Madison, WI, USA
[2]Department of Physical Sciences, School of Science, Technology, Engineering, and Mathematics, Madison Area Technical College, Madison, WI, USA

1. The Antarctic Meteorological Research and Data Center Observational Data Overview

The Antarctic Meteorological Research and Data Center (AMRDC) at the University of Wisconsin-Madison (UW) has managed real-time meteorological data distribution for decades. Much of its data distribution consists of observational data from its Automatic Weather Station (AWS) network, which began in 1980 (Lazzara et al. 2012). Another main portion consists of Antarctic satellite composite imagery, which began at the AMRDC in 1992 (Kohrs et al. 2015). Antarctic meteorological data stewardship and archive have been a priority throughout the AMRDC project, with real-time Antarctic meteorological data made available on the AMRDC website (https://amrdc.ssec.wisc.edu/) and archived data available on the AMRDC Data Repository (Lazzara et al. 2025). This presentation will focus on improvements to real-time AWS data processing and provide updates on real-time data available on the AMRDC website.

2. Improvements to Real-time Argos AWS Processing

In the past few months, the real-time decoding and processing of UW AWS network data utilizing Argos transmissions was updated to improve timeliness and increase the amount of data offered. Argos AWS data are made available via the Argos Data Collection System (DCS), which utilizes polar orbiting satellites to relay data. The AMRDC would historically get Argos AWS data via McIDAS to post real-time. However, there would typically be a 3-4 hour or more delay in data availability. In recent years, the delay increased as changes were made to the polar-orbiting satellites using DCS. To increase timeliness of data availability, a new Argos AWS decode process was established at AMRDC in April 2026 to pull and decode real-time hexadecimal data directly from Woods Hole Group (formerly CLS America), a subsidiary of the Argos program. Figure 1 shows the improved timeliness of Argos AWS availability when the processing was updated.

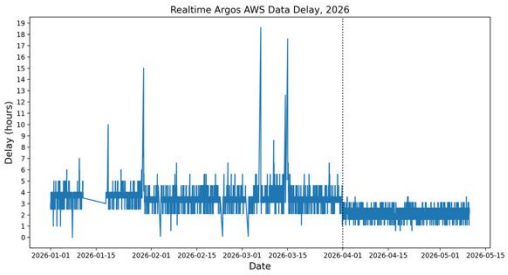

Fig. 1: Time series of real-time Argos AWS delay (hours) from 1 Jan 2026 to 9 May 2026. The vertical dashed black line denotes when processing was updated.

This new Argos processing method allows both for decoded UW AWS data to reach the Global Telecommunication System (GTS) sooner. It also allows for more AWS data to

be processed and made available to the community.

3. Real-time Data on AMRDC website

UW AWS data continue to be made available on the AMRDC website, including text listings, meteorograms, and weather maps. AWS data from other Antarctic groups are also being posted on the website. These include AWS data from the Naval Information Warfare Center (NIWC) network and the McMurdo Long Term Ecological Research (MCM-LTER) network.

Other updates to website data products include Antarctic satellite composite imagery animations and satellite image displays, including Day-Night band imagery from the Visible Infrared Imaging Radiometer Suite (VIIRS) on the Suomi-NPP polar-orbiting satellite (Fig. 2).

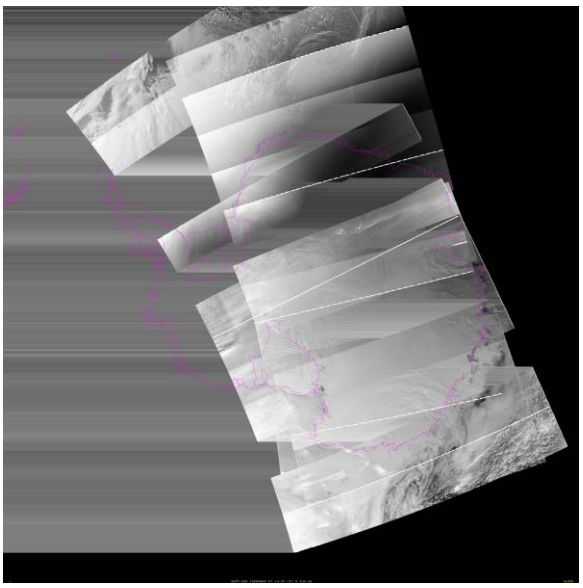

Fig. 2: Day-Night band imagery from Suomi-NPP over Antarctica on 5 June 2026.

4. Conclusions and Discussion

With updated real-time Argos UW AWS processing and updated data sources and displays, our goal at the AMRDC is to make Antarctic meteorological data easily accessible to all. We are open to feedback on how to better organize and make available the various real-time Antarctic meteorological datasets we have on our website. We can work with various groups on providing their data real-time. If groups have Antarctic meteorological datasets they wish to submit or link to on the AMRDC Data Repository, we can work with them on that as well.

5. Acknowledgments

The authors appreciate the support of the National Science Foundation under grant number 1951720 and 2301362 (UW), and 1951603 (MATC).

6. References

Kohrs, R. A., M. A. Lazzara, J. O. Robaidek, D. A. Santek, and S. L. Knuth, 2014: Global satellite composites - 20 years of evolution. *Atmospheric Research*, **135**, 8-34. https://doi.org/10.1016/j.atmosres.2013.07.023.

Lazzara, M., G. Weidner, L. Keller, J. Thom, and J. Cassano, 2012: Antarctic Automatic Weather Station Program: 30 Years of Polar Observation. *Bull. Amer. Meteor. Soc.*, **93**, 1519-1537. https://doi.org/10.1175/BAMS-D-11-00015.1

Lazzara, M. A., M. G. Noojin, K. J. Shannon, D. E. Mikolajczyk, and L. J. Welhouse, 2025: An Antarctic Meteorological Data Repository. *Bull. Amer. Meteor. Soc.*, Accepted. DOI: 10.1175/BAMS-D-24-0178

POLAR POTPOURRI: STATUS AND THE NEAR-FUTURE OF AWS AND AMRDC PROJECTS

Matthew A. Lazzara[1,2,3], Lee J. Welhouse[1,2], David E. Mikolajczyk[1,2], Andy J. Kurth[4], Forbes A. Filip[4], Taylor P. Ziegler[1,2], Sophie Orendorf[1], Jonathan M. Chambers[1,3], Grace O. Zongo[1,5], Mary A. Reinhardt[1,3], Jake A. Zagar[1,3], Linda M. Keller[1,3], and George A. Weidner[1,3]

[1]Antarctic Meteorological Research and Data Center, Space Science and Engineering Center University of Wisconsin-Madison, Madison, WI

[2]Department of Physical Sciences, School of Sciences, Technology, Engineering, and Mathematics, Madison Area Technical College, Madison, WI

[3]Department of Atmospheric and Oceanic Sciences, University of Wisconsin-Madison, Madison, WI

[4]Department of Electrical Engineering Technology, School of Sciences, Technology, Engineering, and Mathematics, Madison Area Technical College, Madison, WI

[5]Department of Electrical Engineering, University of Wisconsin-Madison, Madison, WI

https://amrdc.ssec.wisc.edu
https://amrdcdata.ssec.wisc.edu

1. OVERVIEW

In review of the past year, and looking ahead to the 2026-2027 field season, this simultaneously provides a status report as well as the near future plans of the Antarctic Meteorological Research and Data Center (AMRDC) and Automatic Weather Station (AWS) projects. This includes elements such as the AMRDC Data Repository (ADR; Lazzara et al., 2025), AMRDC data relay/data flow, (e.g., Antarctic-Internet Data Distribution (Ant-IDD), etc.), and a reminder of the World Meteorological Organization (WMO) Integrated Global Observing System (WIGOS). An abbreviated satellite meteorology status report is provided. The upcoming 2026-2027 Antarctic automatic weather station (AWS; Lazzara et al., 2012) field season is outlined along with upcoming activities of the AMRDC project. Feedback from the community is encouraged and welcomed.

2. AMRDC DATA REPOSITORY (ADR)

The ADR has continued steady growth over the past year exceeding 5730 datasets with over 110 linked resources. The ADR has over 500 monthly unique visitors and has aided in the download of 5000 datasets over the past year. Several in the community have deposited data in the ADR. Some loose ends are in progress to complete the availability of some datasets from the old file transfer protocol (FTP) site. Improvements have been made for the visualization of AWS observations and data intake into the ADR. Overall, the success and future of the ADR lays in the hands of this community. As such, use of the ADR as a data source is strongly encouraged, as well as a repository for anyone with data to deposit. The AMRDC offers data to the community via a range of means including web, McIDAS ADDE (Man computer Interactive Data Access System Abstract Data Distribution Environment; Lazzara et al, accepted), Thematic Real-time Environmental Distributed Data Services THREDDS, and Antarctic-IDD.

3. ANTARCTIC-IDD

The sharing of Antarctic meteorological data via the Antarctic-IDD was conceived over 20 years ago at this very meeting in Charleston. Since that time, a full demonstration and operational exchange system has been developed and reliably delivers over 7 to 10 Gb of data per day. Full runs of the Antarctic Mesoscale Prediction System (AMPS) model output, Antarctic composite satellite imagery, and AWS observations are all available in real-time over the network. This is the only

exchange means between the operational and research segments of the US Antarctic Program (USAP). Yet with all of this success, engagement with the Antarctic-IDD is stagnant. Community usage is encouraged (see Figure 1). While it has been established that the underlying framework using Local Data Manager (LDM) is indeed not Internet Protocol version 6 (IPv6) compliant, the future of Antarctic-IDD has means to continue regardless of the transmission software system. Today the World Meteorological Organization (WMO) has organized the WMO Information System version 2.0 (WIS 2.0) that is an assembly of tools that may be a possible future structure for the exchange of data amongst interested users. The AMRDC has plans to begin testing WIS 2.0 in the future.

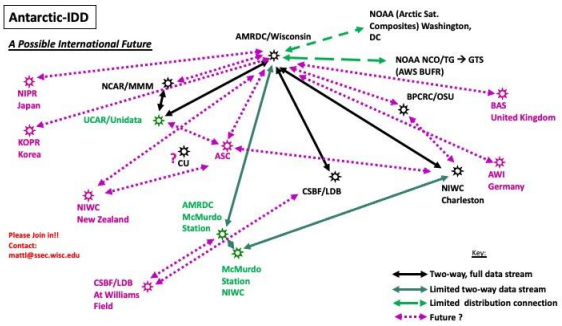

Figure 1. The Antarctic-IDD as envisioned in the future with expanded participation.

4. AWS 2026-2027 FIELD SEASON

Pending arrangements, this coming field season a team of three will be focusing on four elements. The first is the continued servicing of West Antarctic segment of the AWS network. With nearly half of the network serviced last season, this season aims to complete this long overdue effort. The second is the potential installation of a radiation shield test facility at South Pole Station, if field plans can be setup. The third activity is the installation of additional Madison AWS units for comparative testing, as planned years ago. The final task is centered around traditional servicing and repair of AWS sites across the region. Due to limited resources, no work is expected in Adelie Land and Enderby Land over the coming year.

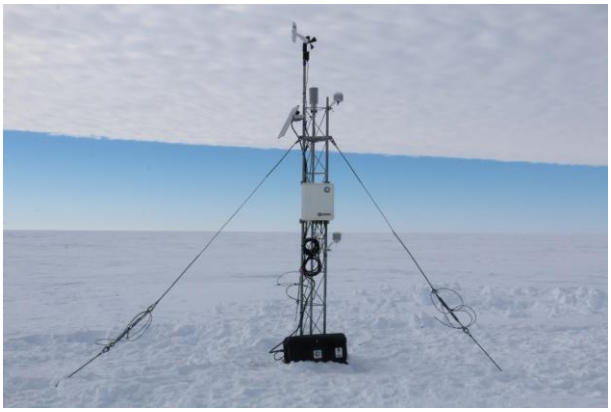

Figure 2. Madison AWS (M-AWS) Skomik, 79.8°South, 170.5°East, is located on the western edge of the Ross Ice Shelf.

5. US ANTARCTIC WIGOS

As the sub-focal point for the WIGOS for the National Science Foundation, efforts over the past 3 years have assigned WIGOS Station Identifiers (WSI) to all currently active Wisconsin and Madison AWS systems, following WMO procedures and conventions. In the coming year, real-time AWS observations distributed via BUFR format will have WSI added, pending arrangements. Additionally, the AMRDC aims to being working with other USAP partners who have WMO identifiers to update their entries in the WMO OSCAR/surface database including having WSI assigned following the NSF WIGOS issue numbering scheme (see figure X). This specifically impacts weather operations at Palmer Station, South Pole Station, and McMurdo Station along with non-Wisconsin/Madison AWS.

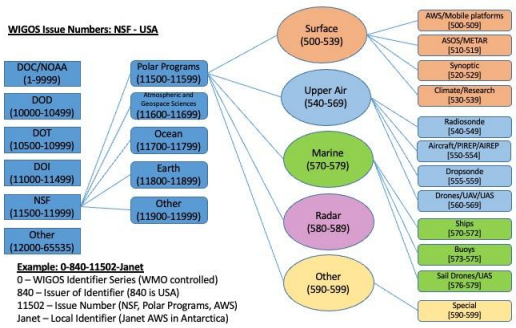

Figure 3. NSF's WIGOS Issue numbers.

6. ANT-RCC and ANT-CF

In the past year, the Antarctic Regional Climate Center (AntRCC) has entered into a formative stage. While formalities are underway, the AntRCC community has engaged in having two Antarctic Climate Forums (AntCF). These bring together Antarctic climate experts, Panel of Experts on Polar and High Mountain Observations, Research and Services (PHORS), members of the Antarctic Advisory (AntAG) group, AntRCC participants, and others in the WMO. Outcomes from the AntCF are to draft a consensus outlook statement regarding temperature, precipitation and other cryospheric variables for the coming months as well as outline impacts across different sectors and gain an understanding of user needs for climate information. More can be learned at the AntRCC's website: https://antarcticrcc-network.org/

7. COMMUNITY INPUT

All topics reviewed here along with the specific missions of the AMRDC and AWS projects demand community input. These efforts are resulting in community assets. Hence, contributing to the group discussions at the workshop are essential. Please bring your ideas, concerns, questions, suggestions and recommendations.

8. ACKNOWLEDGEMENTS

This material is based upon the work supported by the National Science Foundation grant numbers 1951603, 1951720, 2301362, and 2301363.

8. REFERENCES

Lazzara, M. A., G. A. Weidner, L. M. Keller, J. E. Thom, and J. J. Cassano, 2012: Antarctic Automatic Weather Station Program: 30 Years of Polar Observation. *Bull. Amer. Meteor. Soc.*, 93, 1519–1537, https://doi.org/10.1175/BAMS-D-11-00015.1.

Lazzara, M. A., M. G. Noojin, K. J. Shannon, D. E. Mikolajczyk, and L. J. Welhouse, 2025: An Antarctic Meteorological Data Repository. Bull. Amer. Meteor. Soc., 106, E1434–E1438, https://doi.org/10.1175/BAMS-D-24-0178.1.

Lazzara, M.A., R.L. Schaffer, D.A. Santek, J.O. Robaidek, R.A. Kohrs, R. Carp, K. Bedka, L. Nguyen, M-A. Martinez, G. Sebesnste, and B. Shaw, 2026: McIDAS at 50 Years, Bull. Amer. Meteor. Soc., accepted.

AMPS Update – June 2026

Kevin W. Manning and Jordan G. Powers

Mesoscale and Microscale Meteorology Laboratory
U. S. National Science Foundation National Center for Atmospheric Research
Boulder, Colorado, USA

1. INTRODUCTION

The Antarctic Mesoscale Prediction System (AMPS) is a real-time experimental numerical weather prediction (NWP) system focused on Antarctica. Funded by the National Science Foundation to support forecasting needs for the United States Antarctic Program (USAP), AMPS has been producing twice-daily NWP guidance since 2000.

AMPS uses two community models principally developed and maintained at the Mesoscale and Microscale Meteorology (MMM) Laboratory at the NSF National Center for Atmospheric Research (NCAR). The Weather Research and Forecasting (WRF) model has been used in AMPS since 2005, and has been the primary model for AMPS since 2008. AMPS makes use of certain modifications to WRF physics developed at the Byrd Polar and Climate Research Center (BPCRC) of the Ohio State University. In recent years, the Model for Prediction Across Scales (MPAS) has been under testing in AMPS. MPAS is expected soon to replace WRF as the core NWP model in AMPS.

AMPS runs these two NWP models, WRF and MPAS, twice daily on NCAR's supercomputers, with a computing allocation funded by NSF for that purpose. Valuable support for AMPS use of this hardware is provided by NCAR's Computational and Information Systems Laboratory (CISL).

AMPS produces NWP guidance in the form of graphics and tables uploaded to the AMPS web page: https://www2.mmm.ucar.edu/rt/amps. In addition, a subset of model output in the form of GRIB files is made available through the web page and also distributed via the Antarctic Internet Data Distribution (Antarctic-IDD) network. The web page contents are available for a few days before being scrubbed, done because of disk space limitations. AMPS maintains a long-term archive of its graphics and its GRIB subset files, available through NCAR's Geoscience Data Exchange (GDEX), at https://gdex.ucar.edu/datasets/d473002.

2. WRF TO MPAS TRANSITION

WRF has been running in AMPS since 2005, and has been the primary model since 2008 (replacing the older MM5 model in AMPS). WRF is aging software, now nearing end-of-life in the grand cycle of software development. The MPAS model, under active development over the past decade, has become a viable replacement for WRF and is increasingly used by both the research and operational met communities. AMPS has been testing MPAS in parallel with WRF for several years, and the time is approaching for AMPS to shut off WRF and focus on MPAS.

Model development priorities within MMM have shifted from WRF to MPAS. A switch to MPAS in AMPS is advisable, since it assures long-term support of the core model, and development of WRF by MMM is ending. Another motivation for running MPAS as the sole model in AMPS is the computational cost of running two models. Additionally, NOAA has announced plans to adopt MPAS as a central model in their next-generation NWP efforts (https://epic.noaa.gov/noaa-chooses-mpas-to-be-the-next-generation-nws-operational-model), so active community involvement in, and support of, further development of MPAS can be expected. AMPS is well-placed to take advantage of, and contribute to, the growing community momentum behind MPAS.

Two major impediments to a full adoption of MPAS in AMPS have been recently overcome. The first, achieving the high-resolution in MPAS that AMPS delivers with WRF, has been met with an easy method to produce a high-resolution mesh over a region of the globe. This capability, as referenced at last year's WAMC, allows AMPS to offer kilometer-scale MPAS forecasts in the Ross Island region, similar in scale and coverage to the highest-resolution WRF grid offered in AMPS. This mesh has been in place for nearly a year now, and has proven to be a robust addition to the AMPS MPAS suite.

The second difficulty was the production of MPAS graphics for AMPS. While we have had a capability to reformat MPAS output into the form of WRF output files for processing by the WRF-based graphics program (RIP4) used in AMPS, this procedure was unpleasant and ungainly. It requires spatial interpolation, resulting in a

loss of details resolved by the MPAS mesh, and it requires two output reformatting steps, consuming substantial computing time and disk space. Additionally, the WRF-based graphics program is obsolete, and the graphics library it depends on is no longer formally supported. Therefore, a high priority for the past year has been the development of MPAS-native graphics program that can produce the plots that AMPS users are familiar with. This capability now exists in a basic form, coded in Python and using the Matplotlib graphics module for a variety of high-quality, customizable plots. Development of this package is ongoing.

A new element to the MPAS production suite for AMPS is a set of MPAS ensemble products, similar to the WRF ensemble products. AMPS now runs a 5-member ensemble forecast out to five days, initialized by initial conditions from five NOAA Global Ensemble Forecast System (GEFS) members. Initial time-series graphics from the MPAS ensemble are now available, but horizontal charts for this are still in development. More members will be added to this ensemble as WRF computational processes for AMPS are discontinued and the needed compute capacity is available.

An important consideration for routine AMPS availability is a fallback capability for producing AMPS products from MPAS during periods of NCAR supercomputer maintenance and outages. Up to now, the MPAS suite for AMPS has been considered expendable during NCAR supercomputing downtime, with emphasis placed on producing the WRF suite of products. Currently, development is underway for MPAS production on cloud computing resources, which would be used during supercomputer downtime. Additionally, MPAS production on a smaller compute system at NCAR may also be possible for times when NCAR's principal supercomputer is offline.

3. COLD BIAS INVESTIGATIONS

An intermittent yet systematic cold bias in MPAS, described at last year's WAMC meeting, has been investigated in a case study of a particular event. The bias is most prevalent during moderately low wind conditions, in the cold season, especially over the Ross Ice Shelf. This situational bias may be related to a nighttime cold bias seen during the austral summer as well. While these errors are evident in the WRF simulations as well, they tend to be greater in MPAS.

Due to the prevalence of this bias in lighter-wind conditions, sensitivity to PBL mixing parameters was investigated, but little sensitivity was found. Much more sensitivity was seen to snow-layer thermal properties of thermal conductivity and heat capacity as these are represented in the Noah-MP land surface model (LSM). The implementation of Noah-MP in MPAS uses a newer version of the Noah-MP code, and calculation of these thermal properties has been modified and tuned as compared to the older version used in WRF. Reverting these properties to the older procedures as used in WRF appears to mitigate the frequency and severity of these cold forecast events.

Fig. 1 shows an example of station time series for (a) May 2025, before the MPAS modifications, and (b) May 2026, after these changes to MPAS. While comparing results from two different years presents difficulties in interpretation, overall trends at this single site are representative of what can be seen at many sites in the Ross Ice Shelf region at various times of the year. Before the change, the cold bias events are prominent in the MPAS results. After the MPAS code changes, the cold bias events, while still happening, are much less frequent and much less severe.

Other temperature biases remain; particularly evident (and not shown) is an over-amplitude diurnal cycle seen at many sites in the Austral summer season.

4. SUMMARY

With a full transition from WRF to MPAS planned before the 2026/2027 field season in Antarctica, AMPS will return to using a single model for production of its Antarctic NWP guidance. While it may seem disruptive in the short term, this shift is a simplifying step which will reduce computational costs for AMPS, as well as personnel time and energy. Many details remain to be resolved before the transition can be considered complete. Even when the transition is accomplished, development of MPAS, and adaptation of MPAS to the unique needs of AMPS, will continue for many years.

While WRF has served AMPS and the wider NWP community well for over two decades, MPAS is now poised to become the model of choice for many applications worldwide, including weather research, education, and forecast operations. The use of MPAS in AMPS contributes to that community by building knowledge and demonstrating performance of the model in unique and challenging polar environment. AMPS in turn benefits from a broad community committed to active development of a state-of-the-art NWP model.

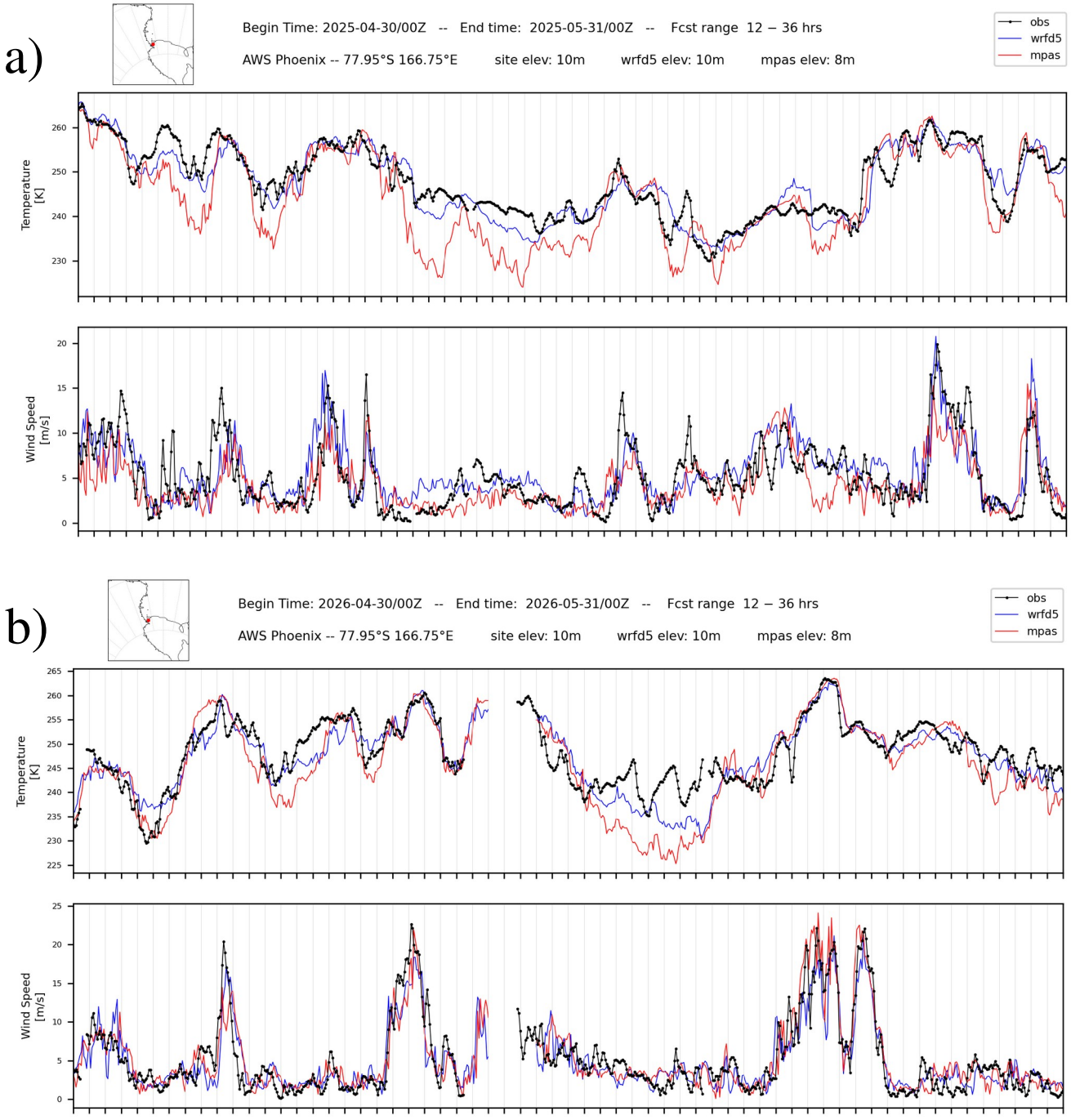

Fig. 1. Temperature and wind speed time series at the site of Phoenix AWS for a) May 2025 and b) May 2026. Observations in black, WRF forecast in blue, MPAS forecast in red. Observations are smoothed over one hour for each hourly point. Model output is from forecast lead times 12-36 hours, with the output from two successive initializations averaged to create approximately continuous time series. May 2025 represents results before modifications to the snow thermal characteristics were introduced to the MPAS code. May 2026 represents results after these modifications were added to MPAS. Observations provided by the Antarctic Meteorological Research and Data Center (AMRDC), a joint project of the University of Wisconsin Madison and Madison Area Technical College.

PERFORMANCE OF POLAR WRF IN THE POLAR REGIONS AND TRANSITION TO A REGIONAL EARTH SYSTEM MODEL

David H Bromwich, Lesheng Bai, Keith M. Hines, Saurav dey Shuvo, and Rui Sun
Byrd Polar and Climate Research Center, The Ohio State University

The polar-optimized version of the Weather Research and Forecasting (PWRF) model is employed globally for investigations of the weather and climate of both polar regions. It has been upgraded to version 4.7.1 with an emphasis on refining the parameters in the Noah-MP land surface scheme and was released on February 27, 2026. The performance of the latest PWRF in both the Arctic and Antarctic is illustrated. Recent enhancements to PWRF include its coupling to the 2-moment Piektuk blowing snow scheme and the MITgcm global ocean model, making the transition to a regional Earth System model. Selected results from blowing snow simulations in North Dakota and atmosphere-ocean coupled simulations for the Southern Ocean are presented.

A POLAR WRF AND UNIFIED MODEL STUDY OF AN ATMOSPHERIC RIVER EVENT AT DAVIS, ANTARCTICA

Keith M. Hines, Sonya Fiddes, Simon Alexander, David H. Bromwich, Mariana Fontolan Litell, Sheng-Hung Wang, and Zhangcheng Pei
Byrd Polar Climate & Research Center

As part of the Southern Hemisphere component to the international Year of Polar Prediction (YOPP-SH), we present a modeling and observational study of an atmospheric river event for coastal East Antarctica during June 2022. The aim is to improve Antarctic weather forecasting, especially during the less-studied winter season. The atmospheric river brings relatively warm, moist air to Davis Station near the Amery Ice Shelf. The event has precipitation and mixed-phase clouds. Precipitation is reduced by sublimation in the relatively dry lower troposphere. The event also features a strong low-level jet parallel to the East Antarctic coastline. In-situ and remote-sensing data are available from Davis. Radiosondes are available at Davis and Zhongshan stations.

We compare mesoscale simulations of the event with the Met Office Unified Model Regional Nesting Suite (UM) and Polar WRF. The latter model uses two grids. These include a 10-km spacing parent grid with 766 by 628 points and a nested grid with 2-km spacing and with 501 by 501 points centered over Davis. The UM has one grid similar to the high-resolution Polar WRF grid. Initial and boundary conditions provided by ERA-5 for both models. Polar WRF uses the two-moment Morrison microphysics with the Vignon adaptation for pristine conditions. The UM uses the new CASIM and is tested with the Vignon adaptation; a sensitivity test shows improved radiative properties but does not increase cloud liquid water content. Polar WRF simulations show much more cloud liquid water than the UM simulations. Both models simulate reduction in precipitation due to sublimation in the lower troposphere. The models well capture the low-level jet, with the UM most accurately resolving the feature. More detailed observations with quantitative measurements of cloud liquid and cloud ice are needed for further improvement of microphysics simulations for austral winter.

EVALUATION OF AI-BASED WEATHER FORECASTS OVER THE SOUTHERN POLAR REGION

Brian Rakoczy, Saurav Dey Shuvo, David Bromwich, Sheng-Hung Wang
The Ohio State University & Byrd Polar and Climate Research Center

Artificial intelligence (AI) based atmospheric models are increasingly being explored as alternatives to traditional numerical weather prediction systems. This study evaluates the performance of four AI forecasting systems, namely Aurora, GraphCast, Pangu-Weather, and FourCastNet. The AI forecast systems examined in this study are heavily trained on ERA5 reanalysis in combination with other numerical weather prediction analyses and forecast datasets. AI model output obtained from the Cooperative Institute for Research in the Atmosphere (CIRA) and the NOAA-GSL. The output is evaluated poleward of 50°S during December 2025 through January 2026 against automatic weather station observations from the Antarctic Meteorological Research and Data Center (AMRDC) and staffed station observations. Forecasts initialized using the GFS analyses and the ECMWF IFS analyses are compared to assess initialization impacts on forecast skill. Forecast verification focuses on key near-surface variables including 2 m temperature, 10 m wind speed, surface pressure, wind direction, and specific humidity. Verification is conducted using twice-daily 00 and 12 UTC initializations with 6-hourly forecasts extending to 240 hours (10 days). Model output is bilinearly interpolated to station locations and compared using RMSE, bias, correlation coefficient, and derived thermodynamic diagnostics. Preliminary results indicate generally skillful performance across all four AI forecasting systems for surface pressure and temperature forecasts, with relatively small variations in error magnitude between models. All forecast systems exhibit common spatial error structures including coastal wind-speed underestimation and enhanced temperature errors near the northern Antarctic Peninsula. Forecasts initialized from IFS analyses generally demonstrate improved performance relative to GFS initialized forecasts. This work provides a benchmark assessment of emerging AI based forecasting systems within the high latitude Southern Hemisphere environment as a complement to traditional numerical weather prediction systems.

Characterization of Drifting and Blowing Snow at Princess Elizabeth Antarctica Station and Validation of the CRYOWRF Model

Lorena Accossato[1], Rainette Engbers[1], Sergi Gonzàlez Herrero[2], Michael Lehning[1,2]

[1]) EPFL - École Polytechnique Fédérale de Lausanne
[2]) WSL Institute for Snow and Avalanche Research SLF

Abstract

Drifting and Blowing Snow (DBS) are wind driven phenomena of snow transport by saltation and suspension, which occur frequently on the Antarctic continent. The occurence of DBS can significantly influence the surface energy and mass balance of the Antarctic ice sheets. Despite their relevance, DBS processes are not fully understood and under-represented in most regional atmospheric and global climate models. In this study, we characterize DBS and validate the CRYOWRF model under the different meteorological regimes at Princess Elisabeth Antarctica (PEA) station.

The study utilizes data from PEA station, which sits in the escarpment zone of Dronning Maud Land, East Antarctica. Sheltering by the Sør Rondane Mountains reduces the strength of the katabatic flow, while PEA remains directly exposed to cyclonic systems approaching from the coast. The station operates a comprehensive atmospheric monitoring system, featuring a Tall Tower AWS, and a set of instruments for DBS observation: a Snow Particle Counter and a FlowCapt, which allow to directly measure mass flux near the surface; a ceilometer, which allows to estimate the suspended snow in the vertical direction (blowing snow); and a vertically pointing Micro Rain Radar, which records precipitating snow. These instruments also provide a valuable set of measurements used for model validation.

The research is conducted in multiple phases. First, following Gorodetskaya et al. (2013), we performed a cluster analysis to classify hourly-averaged meteorological data of years 2024 and 2025 into the three meteorological regimes present at PEA: Cold Katabatic, Transitional Synoptic, and Warm Synoptic. Then, we defined solely drifting snow events (DS, i.e. times when SPC and FlowCapt were detecting snow particle transport, but the ceilometer was not, as the latter does not measure lower level blowing snow) and drifting and blowing snow events (DBS, identified as when all 3 instruments were recording snow transport). For each regime, we assessed DS and DBS frequency of occurrence, surface mass flux intensity, ceilometer blowing snow cloud top height, and the role of concurrent precipitation. Ceilometer data was passed to an adapted version of the blowing snow detection algorithm by Loeb and Kennedy (2021). Finally, we selected one DBS event for each regime, and used this dataset to validate DBS in the CRYOWRF model, which couples the state-of-the-art atmospheric model WRF (the Weather Research and Forecasting model) with the detailed snow cover model SNOWPACK, and includes a blowing snow scheme (Sharma et al. 2023). Initial snowpack conditions were obtained from a separate 30 year spin-up SNOWPACK simulation at continental scale (27 km resolution), interpolated to the model domain via nearest-neighbor.

Our analysis shows that snow transport at PEA station is largely driven by cyclonic activity from the coast, and scales with synoptic forcing. The Warm Synoptic regime, occurring about 30% of the time, is the least frequent, yet it is responsible for the vast majority of transport phenomena (90% of DBS, and 64% of DS events), the largest surface mass fluxes, and the densest and deepest ceilometer plumes; concurrent precipitation amplifies these values further. The Transitional Synoptic regime shows intermediate behaviour, while the Cold Katabatic has overall small snow transport. The three events selected for CRYOWRF simulation are: i) an exceptionally strong katabatic event in May 2024, driven by a low pressure system to the east of the station, that enhanced and channeled the drainage flow though the Sør Rondane mountains; ii) a Transitional Synoptic event in April 2025, caused by a cyclone approaching the coast; and iii) a Warm Synoptic event resulting from a Fujiwhara interaction between the cyclone of event ii) and a second cyclone approaching shortly after. Figures 1 and 2 illustrate the comparison between model results and surface mass flux measurements and the ceilometer's backscatter, respectively. Model validation shows good performance under katabatic conditions, with the highest Pearson correlations for all the considered meteorological variables (with the exception of wind direction, for which r=0.22, surface pressure, potential temperature at two meters, wind speed, and relative humidity had r ranging from 0.55 up to 0.77). Surface snow mass fluxes and and blowing snow's vertical extent also had high Pearson correlation values (respectively ranging from 0.43 to 0.56, and equal to 0.6). Accuracy declines for the Warm Synoptic case, and drops further for the Transitional Synoptic one. This suggests the model does not correctly simulate the location of the synoptic systems, and thus the influence it exerts at the location of PEA. The model exhibits a cold and dry bias, and overestimates wind speed. DBS transport is underestimated due to excessive modeled snowpack cohesion, inherited from the initial conditions, which keeps friction velocity below the saltation threshold.

This study exploits the unique multi-instrument observational setup at PEA station, tying together ground based observations (Gossart et al. 2017, Loeb and Kennedy 2021) to atmospheric models with blowing snow (Sharma et al. 2023,Gerber et al. 2023).To our knowledge, this represents the first attempt to validate blowing snow in its vertical extent.

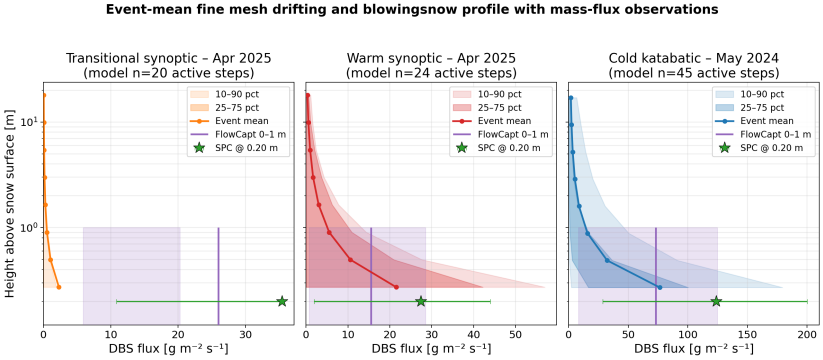

Figure 1: Event mean modeled vertical profiles of drifting and blowing snow (DBS) mass flux [$g\,m^{-}2\,s^{-}1$] as a function of height above the snow surface [m], shown on a logarithmic vertical axis for each simulation. Colored lines indicate the mean flux profiles, dark and light shaded bands show the interquartile range (25th–75th percentile) and the 10th–90th percentile range, respectively. Green stars with error bars show the mean ± IQR of SPC point measurements at 0.20 m. Purple vertical lines and shaded rectangles indicate the mean ± IQR of FlowCapt integrated mass flux in the 0–1 m range

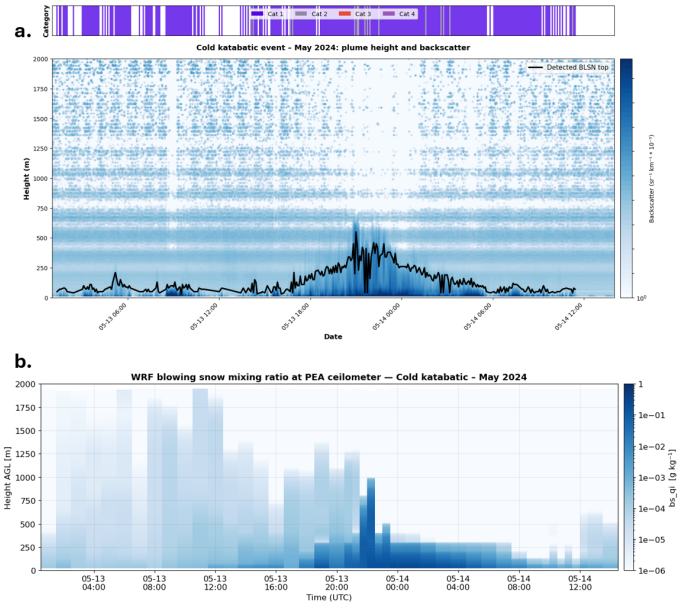

Figure 2: a. Timeheight plot, for the cold katabatic event, of ceilometer backscatter [$10^{-}5\ km^{-}1\ sr^{-}1$]; the bar at the top indicates classification of each 5-minute period according to the blowing snow detection algorithm (Loeb and Kennedy 2021, Gossart et al. 2017), where cat1 = clear-sky blowing snow, cat2 = cloud/precipitation with blowing snow, cat3 = intense mixed event; the black line represents the blowing snow cloud top detected by the same algorithm b. timeheight plot, for the cold katabatic event, of blowing snow mixing ratio from CRYOWRF variable bs_qi ($g\,kg^{-}1$)

References

Gerber, Franziska, Varun Sharma, and Michael Lehning (June 2023). "CRYOWRF—Model Evaluation and the Effect of Blowing Snow on the Antarctic Surface Mass Balance". In: *Journal of Geophysical Research: Atmospheres* 128.12, e2022JD037744. ISSN: 2169-897X, 2169-8996. DOI: 10.1029/2022JD037744. URL: https://agupubs.onlinelibrary.wiley.com/doi/10.1029/2022JD037744 (visited on 02/16/2026).

Gorodetskaya, I. V., N. P. M. Van Lipzig, M. R. Van den Broeke, A. Mangold, W. Boot, and C. H. Reijmer (2013). "Meteorological regimes and accumulation patterns at Utsteinen, Dronning Maud Land, East Antarctica: Analysis of two contrasting years". In: *Journal of Geophysical Research: Atmospheres* 118.4, pp. 1700–1715. ISSN: 2169-8996. DOI: 10.1002/jgrd.50177. URL: https://onlinelibrary.wiley.com/doi/abs/10.1002/jgrd.50177 (visited on 02/19/2026).

Gossart, Alexandra, Niels Souverijns, Irina V. Gorodetskaya, Stef Lhermitte, Jan T. M. Lenaerts, Jan H. Schween, Alexander Mangold, Quentin Laffineur, and Nicole P. M. Van Lipzig (Dec. 2017). "Blowing snow detection from ground-based ceilometers: Application to East Antarctica". In: *The Cryosphere* 11.6, pp. 2755–2772. ISSN: 1994-0424. DOI: 10.5194/tc-11-2755-2017. URL: https://tc.copernicus.org/articles/11/2755/2017/ (visited on 02/16/2026).

Loeb, Nicole A. and Aaron Kennedy (Apr. 2021). "Blowing Snow at McMurdo Station, Antarctica During the AWARE Field Campaign: Surface and Ceilometer Observations". en. In: *Journal of Geophysical Research: Atmospheres* 126.7, e2020JD033935. ISSN: 2169-8996. DOI: 10.1029/2020JD033935. URL: https://agupubs.onlinelibrary.wiley.com/doi/10.1029/2020JD033935 (visited on 04/09/2026).

Sharma, Varun, Franziska Gerber, and Michael Lehning (Jan. 2023). "Introducing CRYOWRF v1.0: Multiscale atmospheric flow simulations with advanced snow cover modelling". In: *Geoscientific Model Development* 16.2, pp. 719–749. ISSN: 1991-9603. DOI: 10.5194/gmd-16-719-2023. URL: https://gmd.copernicus.org/articles/16/719/2023/ (visited on 02/16/2026).

ANTARCTIC WINTER NUMERICAL FORECAST IMPROVEMENT FROM ENHANCED SOUTHERN HIGH-LATITUDE RADIOSONDES DURING THE YEAR OF POLAR PREDICTION – SOUTHERN HEMISPHERE (YOPP-SH) WINTER CAMPAIGN

Mariana Fontolan Litell, David H. Bromwich, Jordan G. Powers, Kevin W. Manning, and Sheng-Hung Wang
The Ohio State University

Southern Ocean weather forecasts exhibit lower predictive skill compared to other regions of the planet, in part due to limited conventional observations. The Year of Polar Prediction in the Southern Hemisphere (YOPP-SH) aims to improve weather prediction for Antarctica and the Southern Ocean. The project is centered around the winter Special Observing Period (SOP) that spanned April 15 - August 31, 2022. During the SOP, seven Targeted Observing Periods (TOPs) featured extra radiosonde launches to capture intense weather events, such as major oceanic cyclones and atmospheric rivers. To investigate the impact of these extra radiosondes in numerical weather prediction, NSF NCAR performed experiments using Polar WRF in the Antarctic Mesoscale Prediction System (AMPS) framework. Two different simulation methodologies were performed. The first consisted of assimilating the standard set of observations into the initial conditions for Polar WRF, and these simulations are termed Routine. The second consisted of assimilating in addition to the standard observations, the extra radiosondes from the TOPs, called Extra. Two data assimilation approaches were used: Multi-Resolution Incremental-Four Dimensional Data Assimilation (MRI-4DVAR) and Three Dimensional Ensemble Variational Data Assimilation (3DEnVAR). The forecasts generated covered all the seven TOP periods, starting at each 0000 UTC and 1200 UTC and had a duration of 5 days.

To quantify the benefits of the additional soundings during the TOPs, statistical analyses on Polar WRF forecast runs that were initialized using both MRI-4DVAR and 3DEnVar were performed. These were generated for both forecasts (Extra and Routine) and were validated against ECMWF 5th generation reanalysis (ERA5) for geopotential height, temperature and wind speed, throughout the troposphere and lower stratosphere. Another metric used in this study was the Total Energy Error (TEE).

The extra soundings improve model forecast skill across the Southern Ocean. The positive impacts are particularly pronounced at latitudes south of 60°S, aligning with the findings from the austral summer YOPP-SH campaign. Differences between the data assimilation methods indicate that 3DEnVar tends to produce larger improvements at early forecast times, while MRI-4DVAR the improvement is more persistent at later stages. The Extra forecasts also improve the reperesentation of key meteorological events, such as atmospheric rivers and cyclones.

Increasing the availability of high-quality observations is essential for improving forecast accuracy and advancing our understanding of polar atmospheric processes. Overall, enhancing the atmospheric representation of the Southern Ocean can provide several benefits, including improvements in mid-latitude forecasts and better safeguarding of personnel at the Antarctic

stations. These results highlight the importance of continuing and expanding targeted atmospheric observing efforts across Antarctica.

MPAS-A PERFORMANCE IN THE POLAR REGIONS

David H Bromwich, Lesheng Bai, Qian Xu
Byrd Polar and Climate Research Center, The Ohio State University

The Model for Prediction Across Scales (MPAS) is being run for the Antarctic and Arctic. Version 8.3.1 is employed and considerable effort has been expended to revise the Noah-MP LSM parameters to minimize the land surface temperature biases. In addition, the sea ice model in MPAS has been modified to add specified sea ice albedo, snow depth on sea ice, and sea ice thickness options to the namelist to reduce the sea-ice temperature bias for different seasons. This poster reports on the predictive performance of the revised model against (ERA5) surface and upper air observations.

Analysis of an Antarctic Atmospheric Mass Loss Event

Jordan G. Powers

Mesoscale and Microscale Meteorology Laboratory
NSF National Center for Atmospheric Research
Boulder, Colorado, USA

1. INTRODUCTION

Within a week from June to July 1988, surface pressures over the whole of Antarctica dropped significantly (10's of mb). Occurring in the context of the Semiannual Oscillation (SAO) of the Southern Hemisphere, the surface pressure (SFP) changes were observed in conjunction with low-level outflows from large segments of the continent. Those conditions reflected strong offshore cyclones amplifying climatological katabatic flows, particular the Ross Ice Shelf Air Stream (RAS). The result was a period of atmospheric mass loss for the SH high latitudes.

This event was revealed by Parish and Bromwich (1998) (hereinafter PB98), who investigated it using information available at the time, in particular an ECMWF (European Center for Medium-Range Weather Forecasting) reanalysis dataset. They documented the SFP changes over the continent and into the mid-latitudes and described conditions of the episode.

The current work revisits this case through contemporary model and data-based tools, namely the Model for Prediction Across Scales (MPAS) (Skamarock et al 2012) and ERA5 reanalyses (Hersbach et al. 2020), neither of which existed at the time of the original study. On the modeling side, MPAS is a global atmospheric model, and it offers to capture the scale of this event fully, without the constraints and artifacts of numerical lateral boundaries, such as those of limited-area models like WRF. For many years MPAS has been applied for forecasting in the Antarctic Mesoscale Prediction System (AMPS), a real-time numerical weather prediction capability for Antarctica and the high southern latitudes for the U.S. Antarctic Program (Powers et al. 2012). Thus, MPAS has a record of being relied on for Antarctic atmospheric simulations. On the data side, ERA5 provides the current best-available global atmospheric gridded reanalysis dataset. This has an approximately 31-km horizontal grid equivalent, compared to the 277-km (2.5-deg) ECMWF analyses applied by PB98.

MPAS is applied here to examine the atmospheric conditions and evolution of the Antarctic mass loss event of June 1988, with ERA5 providing a means for large-scale model verification. Here, MPAS's ability to capture the basics of the observed case is shown first, and then the model output used to analyze the event's mechanisms. Some figures from PB98 are reproduced here to provide the observational background, and credit is given PB98 on their original work.

2. MODEL CONFIGURATION

MPAS Version 8.2.3 is run in a global configuration with a refined mesh area over Antarctica and the Southern Ocean. The variable-resolution mesh has a finest spacing of 8 km over Antarctica, coarsening to 48 km northward of the SH mid-latitudes. Figure 1 gives an example of a regionally-refined MPAS mesh over Antarctica, but in this rendition the cells are much larger than those of the actual mesh, because the real mesh cells would be too small to be distinguished in a plot this size.

MPAS is configured with 51 vertical levels and a top at 30 km. The set of physics schemes run, listed in Tab. 1 below, is designated as the "Mesoscale Reference Suite" for MPAS.

Table 1: Physics Schemes
Microphysics: WSM6
Convection: nTiedke
PBL: YSU
LSM: Noah-MP
Surface layer: Revised Monin-Obukhov
Radiation: RRTMG LW/SW
Gravity wave drag: YSU GWDO

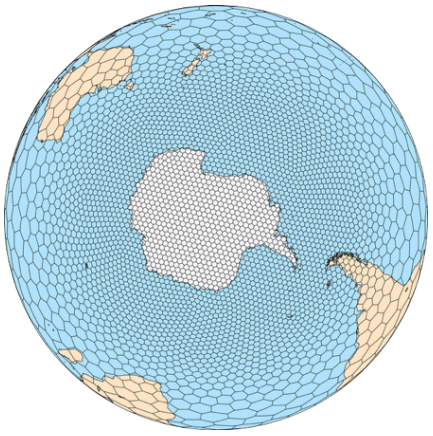

Fig. 1: Example of MPAS global mesh with regional refinement (i.e., smaller mesh spacing) over Antarctica. The mesh shown is coarser than the one

run, which would present cells too small to be clearly visible.

Model initial conditions (ICs) are produced from the ERA5 reanalysis for 12 UTC 27 June 1988. The simulation runs 156 hours, from 12 UTC 27 June to 00 UTC 4 July 1988. No separate additional data assimilation step was done for the MPAS simulation.

3. CASE BACKGROUND

The event centered on 28 June–3 July 1988, the period of largest surface pressure (SFP) decreases over the continent. Work prior to PB98 found that prominent seasonal variations in surface pressure occurred over Antarctica in a cycle dubbed the Semiannual Oscillation (SAO) (see, e.g., van Loon 1967, Schwerdtfeger 1967). The SAO's SFP oscillations reflect variations in the midtropospheric temperature gradients between the middle and high latitudes, the shifts in locations of the circumpolar trough resulting from this baroclinicity, and the resultant fluctuations in synoptic pressure forcings of the trough on the polar continental area. Manifestations of the latter conditions appear in variations in off-continent katabatic flows.

PB98 began their case analysis with considering the persistent katabatic flows off the Antarctic land mass. They recognized that these implied mass transport at low levels, with mass moving toward the subpolar latitudes. Given continuity constraints, however, a subsequent return flow, occurring in the mid-to-upper troposphere, was to be expected. Together the lower- and upper-level mean flows yielded an average meridional circulation. The June 1988 event, however, appeared to reflect a disruption of this pole-midlatitude direct circulation that has historically been seen as a polar component of the global general circulation.

While the SAO's seasonal changes in surface pressure are climatological and statistical, the June 1988 case demonstrates that episodes of abrupt, continental SFP change can be superimposed on a subcycle. Figure 2 presents PB98's depiction of the differences in surface pressure (SFP) over a 48-hr subperiod of the event, 00 UTC 29 June–00 UTC 1 July, based on the ECMWF 2.5-degree dataset. From this, maximum SFP decreases of >18 mb emerged over Marie Byrd Land and the Siple Coast, while decreases of >8 mb extended across West Antarctica and the Plateau.

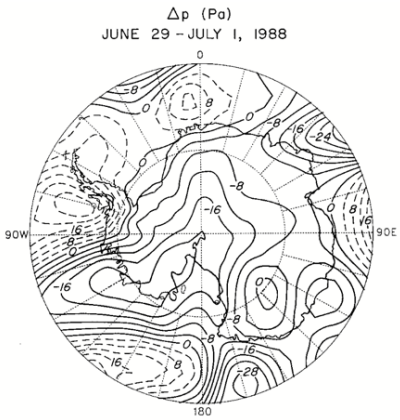

Fig. 2: Surface pressure changes (mb) over the period 00 UTC 29 June–00 UTC 1 July 1988, from PB98. Contour interval 4 mb; solid= pressure decreases; dashed= pressure increases.

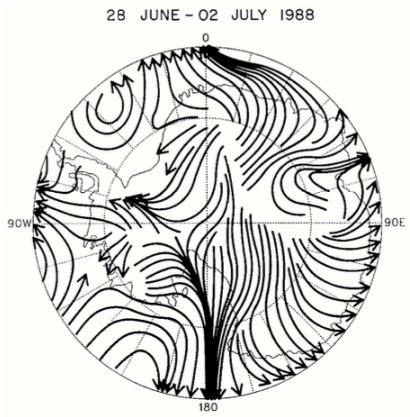

Fig. 3: Analysis of streamlines of surface winds averaged over the period 00 UTC 28 June–00 UTC 2 July 1988 from PB98.

A surface wind analysis of the event from PB98 (Fig. 3) shows the predominate off-continent winds, with a pronounced Ross Ice Shelf Air Stream (RAS) (Parish et al. 2006) around 180E, as well as offshore flows across East Antarctica. The strong RAS is in response to a deep low pressure system north of the Ross Sea that persists through the period. The SLP analysis from ERA5 for 00 UTC 29 June (Fig. 4(a)) shows this cyclone (964 mb), highlighted in yellow. The MPAS simulation reproduces this (Fig. 4(b)), where the central pressure of 966 mb is close to the analyzed value. Figure 4 also reveals lows off of Queen Maud Land (0 E) and East Antarctica (90 E) that are contributing to the offshore flows, and low-level mass transports, from those sectors. MPAS's accurate simulation of these cyclones shows that it has captured some important synoptic elements driving the low-level flows.

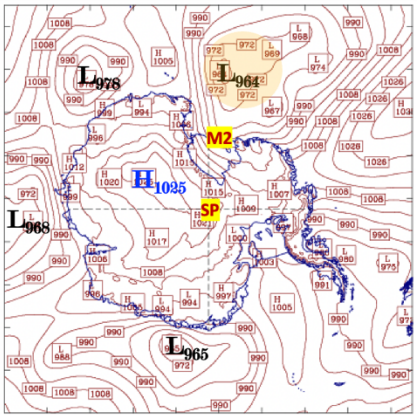

(a)

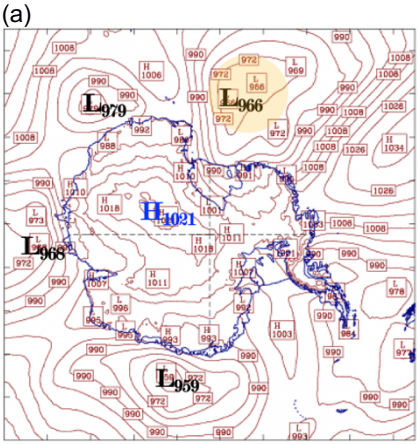

(b)

Fig. 4: SLP analyses for 00 UTC 29 June 1988. Contour interval= 6 mb. Cyclones driving low-level, off-continent flows seen in the northern Ross Sea (150–180W, highlighted in yellow) as well as off East Antarctica (near 90E) and Queen Maud Land (near 0 E). In (a) "SP" and "M2" mark South Pole and Martha II AWS sites referred to in text and shown in Fig. 6. (a) ERA5. (b) MPAS (hr 36).

4. MODEL RESULTS

As noted, motivations in this investigation are to apply contemporary tools to explore this event and ultimately to clarify its evolution and mechanisms. While Fig. 2 presents PB98's analysis of SFP loss from the dated ECMWF 2.5-deg resource, Fig. 5(a) shows the counterpart SFP changes derived from ERA5 reanalyses (.25-deg/31-km). Notable differences from the original analysis are: (i) a much greater SLP loss for the given period—32 mb compared to 20 mb— and (ii) a broader region of highest SFP loss, emerging as two lobes around Pole. Here the generational advance in reanalyses reveals a quantitatively different event, one of higher widespread amplitude.

Figure 5(b) presents the SFP changes from MPAS. Its Antarctic maxima are -32 mb and -20 mb, and the positions and magnitudes of the maxima are verified by the ERA5 results in Fig. 5(a). The largest difference is in the area of pressure decrease off the continent along about 225W (lower left quadrant of plot). Overall, MPAS does succeed in reproducing the large SFP decreases that characterized the event. Furthermore, the accuracy of the MPAS simulation would not have been realized by relying on the older ECMWF-based depiction. Thus, the application of the modern tool of the ERA5 has improved our picture of this event.

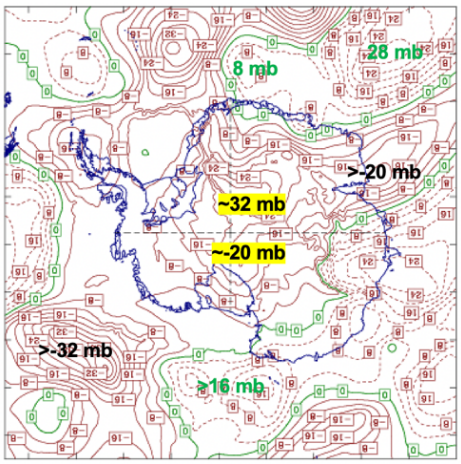

(a)

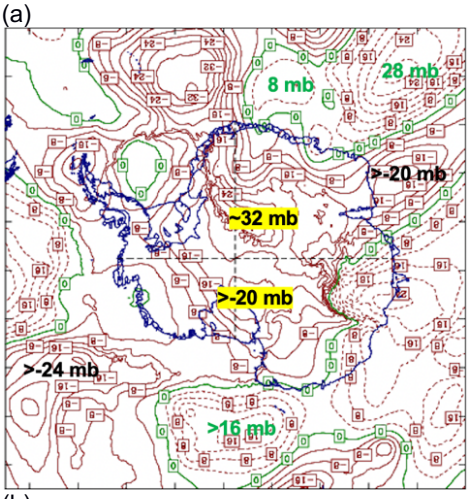

(b)

Fig. 5: SFP differences for the period 00 UTC 29 June–00 UTC 1 July 1988. Solid contours= increases; dashed contours= decreases; zero contour green; interval= 4 mb. Local extrema labeled, with the maxima over Antarctica highlighted in yellow. (a) ERA5. (b) MPAS.

Point observations also verify the MPAS simulation. Figure 6 presents the AWS records for the South Pole and Martha II (Ross Ice Shelf) stations (locations marked in Fig. 4(a)). At South Pole (Fig. 6(a)), the simulation tracks the observation, but has a lesser overall pressure fall (-21 mb MPAS v. -26 mb obs). At Martha II on the northern edge of the Ross Ice Shelf, the model matches the magnitude of the observed decrease of 41 mb. Other sites, not shown, confirm

that MPAS replicates the observed mass losses at points across the continent.

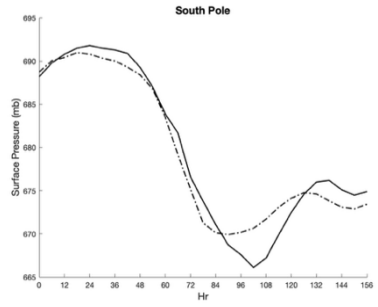

(a)

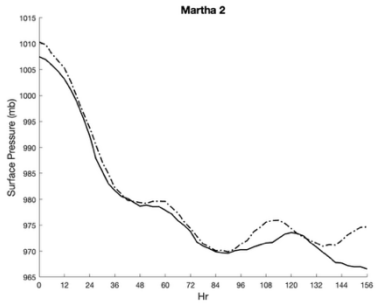

(b)

Fig. 6: AWS (solid line) and MPAS simulation (dot-dashed line) surface pressures (mb) for the period 12 UTC 27 June–00 UTC 4 July 1988 for South Pole and Martha II sites. Hr= Hour after 1200 UTC 27 June. Locations of South Pole and Martha II sites marked in Fig. 4(a). (a) South Pole (90S,0E). (b) Martha II (-78.4S, 173.4W).

Analyses of zonal SFP changes from the pole to the tropics reveal mass adjustment variation with latitude and an overall large-scale mass transfer. As noted by PB98, net SFP decreases, reflected in zonally-averaged changes, are seen over the continent, while increases appear into the midlatitudes. Figure 7 shows the latitudinal SFP changes in ERA5 and MPAS for selected latitudes for the period 00 UTC 28 June–00 UTC 4 July: 86S, 76S, 64S, 58S, 48S, 34S, and 20S. Both ERA5 and the simulation show large pressure decreases (e.g., >20 mb) over all of the continent latitudes (Figs. 7(a)–(c)). At 86S the maximum decreases are -21 mb (ERA5) and -22 mb (MPAS) (Fig. 7(a)). While MPAS shows up to 4 mb greater SFP decreases than ERA5 at 76S (Fig. 7(b)), it does reproduce the trend seen in the observations. The ΔSFP overestimation by MPAS is gone by 64S (Fig. 7(c)), and MPAS simulates the actual averaged SFP change at that latitude.

Both ERA5 and MPAS point to a narrow zone of inflection of the SFP change, ~58S (ERA5)–60S (MPAS) (Fig. 7(d)). At 58S, for example (Fig. 7(d), ERA5 still shows a slight pressure decrease for the period, while MPAS shows a slight gain. Around this zone there are averaged SFP pressure decreases occurring to the south and increases occurring to the north.

A first example of the regime of SFP increases north of this zone is presented in Fig. 7(e) for 48S. Here MPAS almost exactly matches the ERA5-based ΔSFP evolution. The simulation fidelity carries to 34S in Fig. 7(f), which also reveals that the magnitude of the SFP increase is decreasing as one moves northward.

Finally, Fig. 7(g) presents the picture for 20S, in the tropics. Here there is still a net pressure gain for the event, although the increase disappears in the latitudes just to the north (not shown). This reveals that the mass transport from Antarctica has reached the tropics: the event is one of hemispheric impact.

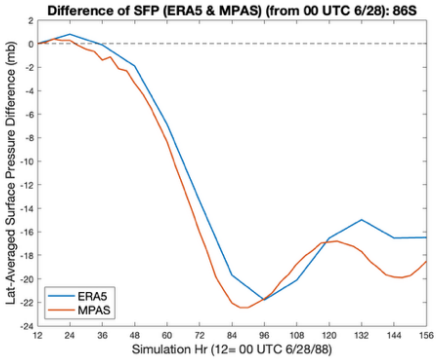

(a)

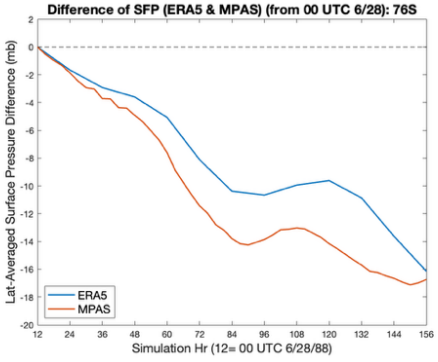

(b)

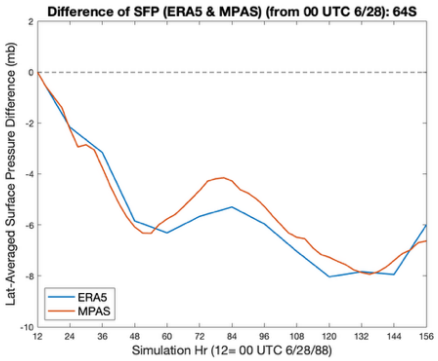

(c)

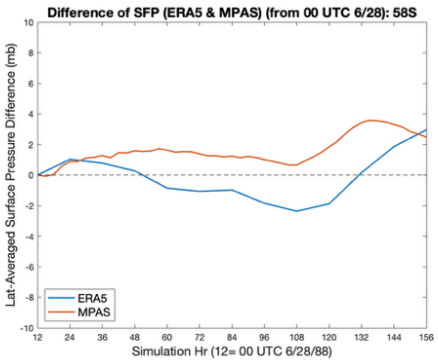

(d)

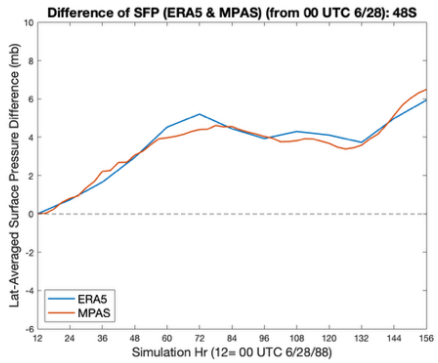

(e)

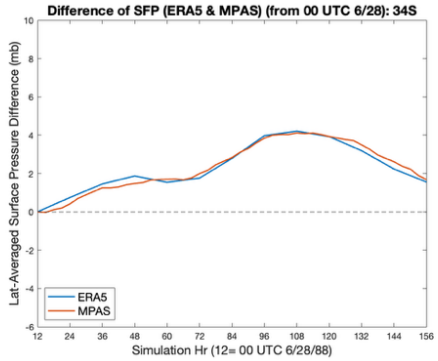

(f)

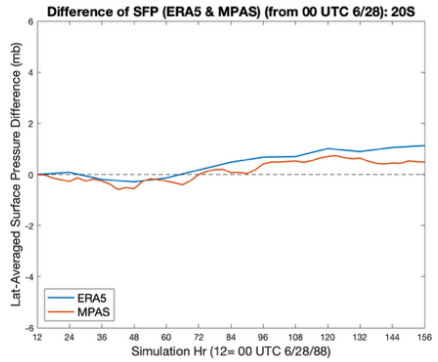

(g)

Fig. 7: Zonally-averaged surface pressure changes (mb) for different latitudes for the period 00 UTC 28 July–00 UTC 4 July 1988 from ERA5 (blue) and MPAS (orange). (a) 86S. (b) 76S. (c) 64S. (d) 58S. (e) 48S. (f) 34S. (g) 20S.

Integrating the changes in zonally-averaged SFP over the event northward from Pole can quantify an aggregate signal of mass changes over the hemisphere. Here, the integrated SFP change for a given latitude is formulated as:

$$\text{IΔSFP} = \int \Delta p \cos\varphi \, d\varphi$$

where Δp= latitudinally-averaged SFP change for a latitude, φ= latitude, and, for 2-degree latitude bins dφ= 2 deg.

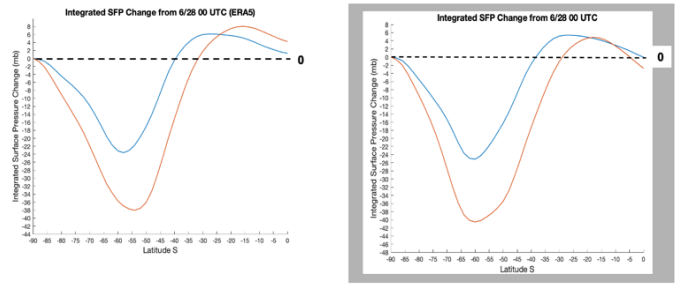

(a) (b)

Fig. 8: Integrated latitudinally-averaged SFP changes (mb) for periods 00 UTC 28 June to 00 UTC 30 June (blue) and 00 UTC 28 June to 00 UTC 2 July (orange). (a) ERA5. (b) MPAS.

Figure 8 shows such integrated changes for two periods of the event: 00 UTC 28 June–00 UTC 30 June (blue curves) and 00 UTC 28 June–00 UTC 2 July (orange curves). For the former period, ERA5 reveals a maximum integrated SFP decrease of -24 mb located at 58S (Fig. 8(a)), while MPAS simulates -25 mb at 60S (Fig. 8(b)). These are the latitudes of inflection of the SFP changes discussed above. The crossover latitude for ERA5, where the integrated SFP becomes positive, is 40S, and MPAS reproduces this result. North of this latitude, the integrated changes become positive, indicating that the Antarctic mass has been transported to the north. The maximum integrated SFP increases for this period are 6 mb from ERA5 and 5.5 mb from the simulation. In addition, one can see that the integrated gains carry into the tropics. This provides another view of the event's hemispheric reach.

For the latter period, ending 00 UTC 2 July, ERA5 shows a maximum integrated mass loss of -38 mb, occurring at 60S, while the simulation produces -40 mb, verifying at the latitude of 60S. For the transition latitude to an integrated increase for this period, ERA5 finds it at 31S, with MPAS showing 30S. The maximum integrated SFP change from ERA5 is +7.5 mb, occurring in the tropical latitudes. MPAS has less of an integrated gain, 5 mb, but that maximum is placed as in the reanalyses.

In summary, MPAS reproduces the ERA5's maximum integrated SFP decreases through very similar

transition latitudes. MPAS also shows the integrated gains occurring over the same lower latitudes, although with a smaller maximum gain. Importantly, MPAS does reproduce the positive values of integrated SFP change well into the tropics revealed by ERA5.

For the SFP decreases to reflect transport from Antarctica, there should be net northward mass fluxes in the event period. As suggested in Fig. 4, the off-continent flows felt the strong lows north of the continental margin, amplifying the climatologic katabatics. The RAS was particularly influenced, and Fig. 9 visualizes this. This plot shows the low-level (.25-km AGL) flow as the SFP signals were emerging. The RAS is circled in blue, and the low northeast of the Ross Ice Shelf is enhancing it. This MPAS-simulated RAS is a high-resolution version of the averaged surface flow during the event from the PB98 ECMWF-based analysis shown in Fig. 3. In addition, other areas of continental outflow appear in conjunction with the cyclones off of Adelie land and Queen Maud Land.

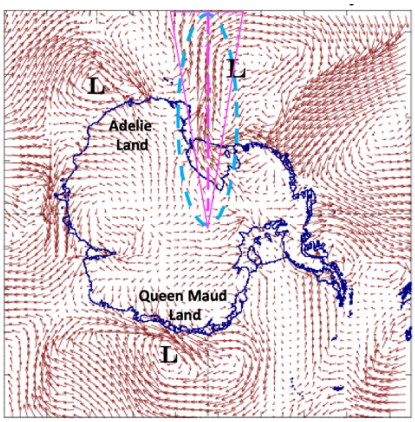

Fig. 9: .25-km AGL flow from MPAS simulation for 00 UTC 29 June 1988. Blue dashed circle marks main RAS corridor. Magenta wedge outlines the region of the averaging of wind fields for the cross-sections shown in Fig. 10; dashed line is the center longitude of the averaged transects, 180E.

To examine the flow vertically, Fig. 10 presents cross-sections through the Ross Ice Shelf sector, composited for transects every 2.5° longitude from 172.5E to 202.5E and all running from 90S to 50S. The composite for the event period of 12 UTC 28 June–12 UTC 1 July 1988 (Fig. 10(a)) reveals some of the well-known Antarctic direct circulation, but the branches of interest here are the strong low-level northward (off-continent) flow and the southward, return flow aloft. Revealing the difference in these event conditions compared to those before the event, Fig. 10(b) shows how the circulation evolves to a circulation that results in mass loss from the continent. This presents the difference in the average circulation of the event period minus that of the pre-event period. While compared to the pre-event period the event period continues to have low-level katabatic and off-continent flow, aloft the return flow is significantly reduced. This change means uncompensated return flow and thus a net mass transport northward, with the result being the reduction in surface pressures over Antarctica.

To quantify the indications from the cross-sections, the mass fluxes off the continent can be calculated from the MPAS output. The integrated longitudinal mass flux for columns averaged around a latitude circle, and weighted by latitude, may be evaluated as follows:

$$\textbf{Mass Flux} = \overline{\int_0^{Top} v(z)\rho(z)\cos\varphi \; dz}$$

where v= northward component of the wind for a model layer, ρ= average density for the layer, φ= latitude, and dz= layer depth. The overbar represents the averaging of the individual column-integrated mass fluxes for all model points in the latitude circle.

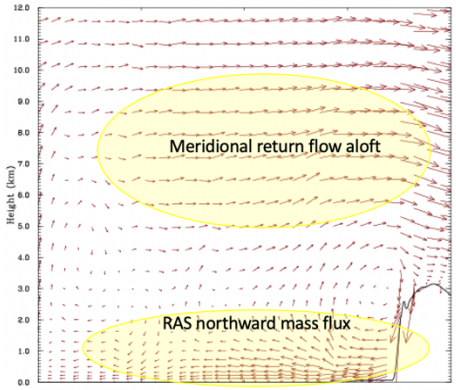

(a)

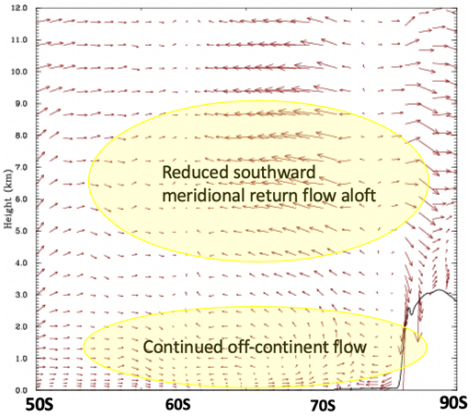

(b)

Fig. 10: Cross-sections of flow in Ross Ice Shelf sector. Flows shown are averages along meridians from 172.5E–202.5E (every 2.5°) and from 90S to 50S. (a) Average flow during period 28 June–1 July. (b) Difference of flows for event period (average for 28 June–1 July 1988) minus pre-event period (12 UTC 27 June 1988).

Figure 11 shows the averaged integrated mass flux (AIMF) for all latitudes from Pole to Equator. Here, positive AIMFs represent northward net fluxes (i.e., supporting continental mass loss) at the given latitude and negative values represent southward net fluxes. Before the event (Fig. 11(a)), there was no consistent integrated mass flux direction for the continental latitudes; net fluxes were variable: northward to 84S, then southward to 70S, then northward to 60S and beyond. However, during the event (Fig. 11(b)) they became consistently northward for all continental latitudes, with magnitudes over three times those of beforehand. Thus, the net mass transport turned off-continent, consistent with the signals of SFP decreases (atmospheric column mass losses) for all latitudes south of ~60S shown earlier.

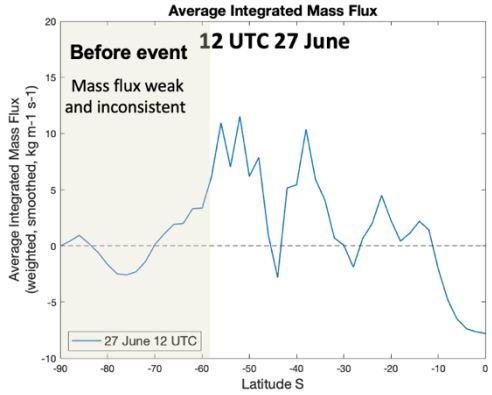

(a)

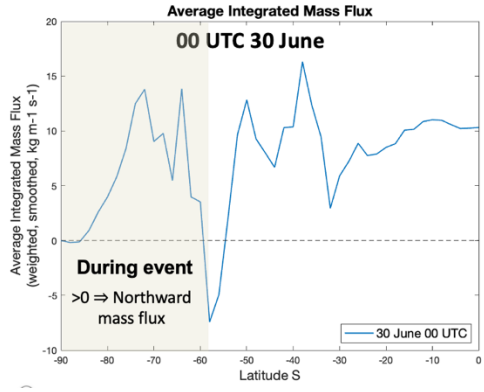

(b)

Fig. 11: Average integrated mass flux (AIMF) (kg m^{-1} s^{-1}) for the pre-event (a) and event (b) periods. AIMF calculated as described in text. Latitudes poleward of 58S highlighted. (a) 12 UTC 27 June 1988. (b) 00 UTC 30 June 1988.

Figure 12 isolates the differences in AIMF between the event and pre-event periods. The change in integrated mass fluxes for all high latitudes is positive (northward) for the event. Thus, the event period was characterized by net northward mass fluxes, with a net off-continent mass transport established. This forced the observed SFP decreases.

The fluxes became relatively northward, too, for 54S–36S and southward for 36S–12S. This implies a period of mass convergence in the mid-latitudes to subtropics, which would result in the SFP increases seen for these zones of the hemisphere (see, e.g., Figs. 7(e)–(g)).

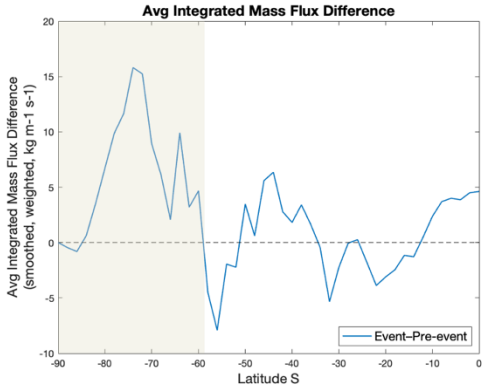

Fig. 12: Differences in average integrated mass flux (AIMF) (kg m^{-1} s^{-1}) for the event minus pre-event periods. AIMF calculated as described in text. Event period values are averages of output every 12 hours from 12 UTC 28 June–12 UTC 30 June 1988. Pre-event period values are time averages for 00 and 12 UTC 27 June 1988. Latitudes poleward of 58S highlighted.

4. SUMMARY

Seasonal fluctuations in average surface pressures over Antarctica define the SAO, the climatological semi-annual procession of pressure evolution over the high southern latitudes. Within the SAO's cycles, however, there can be episodes of dramatic, rapid continent-wide SFP drops reflecting short-term significant atmospheric mass loss. Parish and Bromwich (1998) [PB98] were the first to examine one of these, a case from June 1988. The current study applies tools not available to PB98 for a new look at the case, the Model for Prediction Across Scales (MPAS) and ERA5 reanalyses. Here MPAS is run at high resolution to investigate the event's conditions and mechanisms, with ERA5 providing a modern benchmark for diagnosis and model verification.

The June 1988 event was marked in AWS observations by surface pressure (SFP) falls, and the coarse ECMWF datasets used by PB98 indicated synoptic-scale decreases of >-20 mb over a few days. The MPAS simulation captures continent-wide SFP decreases over a 4–5-day period, but with notably greater amplitudes than previously identified. ERA5 confirms MPAS's estimates of regional 32 mb pressure decreases. For zonally-averaged SFP changes across latitudes from the Pole to the Equator, the MPAS output shows in detail the magnitude and timing of decreases over the continental latitudes, transitioning to increases from north of ~60S into the subtropics, with ERA5

confirming the simulation. Integrated metrics of SFP change reveal that the mass fluxes project well into the SH tropics, and thus the event is of hemispheric impact.

Analyses from ERA5 and MPAS show strong low-level outflows in three main areas: the Ross Ice Shelf (RAS), Adelie Land, and Queen Maud Land. In these regions katabatic off-continent flows are amplified by the pressure gradients of strong cyclones offshore. Aloft, it is seen that the return flow to Antarctica reduces during the event period compared to the pre-event period, and thus the normally-compensating poleward mass transport cannot match the equatorward flow below. The reason for this temporary condition is not yet known.

MPAS reveals that the SFP changes are a product of net column-integrated mass flux off of the continent (i.e., northward); the simulation produces a clear shift to net northward integrated mass fluxes moving from the pre-event period through the event. Thus, this Antarctic episode is a consequence of enhanced, unbalanced equatorward mass fluxes. MPAS in conjunction with ERA5 confirm in large part the view presented originally by PB98, but the new datasets reveal more of the mechanisms and conditions of this notable event.

ACKNOWLEDGEMENTS

The author thanks the NSF Office of Polar Programs for its support of AMPS. The author acknowledges the prior seminal study of Parish and Bromwich (1998).

REFERENCES

Hersbach H., and Co-Authors, 2020: The ERA5 global reanalysis. *Quart. J. Royal. Meteor. Soc.*, **146**, 1999–2049. https://doi.org/10.1002/qj.3803

Parish, T.R., and D.H. Bromwich, 1998: A case study of Antarctic katabatic wind interaction with large-scale forcing. *Mon. Wea. Rev.*, **126**, 199–209.

Parish, T.R., J.J. Cassano, and M.W. Seefeldt, 2006: Characteristics of the Ross Ice Shelf air stream as depicted in Antarctic Mesoscale Prediction System simulations. *J. Geophys. Res. Atmospheres*, **111** (D12), 12109–12120. https://doi.org/10.1029/2005JD006185

Powers, J.G., K.W. Manning, D.H. Bromwich, J.J. Cassano, and A.M. Cayette, 2012: A decade of Antarctic science support through AMPS. *Bull. Amer. Meteor. Soc.*, **93**, 1699–1712.

Schwerdtfeger, W., 1967: Annual and semi-annual changes of atmospheric mass over Antarctica. *J. Geophys. Res.,* **72,** 3543–3547.

Skamarock, W. C., J. B. Klemp, M. G. Duda, L. Fowler, S.-H. Park, and T. D. Ringler, 2012: A multi-scale nonhydrostatic atmospheric model using centroidal Voronoi tessellations and c-grid staggering. *Mon. Wea. Rev.*, **240**, 3090–3105. doi:10.1175/MWR-D11-00215.1

van Loon, H., 1967: The half-yearly oscillations in the middle and high southern latitudes and the coreless winter. J. Atmos. Sci., **24**, 472–486.

MARCH 2022 EAST ANTARCTIC HEATWAVE UNDER DIFFERENT BACKGROUND CLIMATE CONDITIONS

Xun Zou, Edward Blanchard-Wrigglesworth, Zhenhai Zhang, Matthew R. Mazloff, Benjamin Moore, Dan Lubin, Matthew A. Lazzara, Irina V. Gorodetskaya, Jason M. Cordeira, Matthew Simpson, Brian Kawzenuk, Jinxi Li, Lanhao Yang, Penny M. Rowe, F. Martin Ralph
Scripps Institution of Oceanography

East Antarctica experienced an unprecedented heatwave in March 2022 driven by a strong atmospheric river (AR). Using high-resolution model simulations, this study examines how external forcings influence AR development and associated surface impacts during the event. Changes in both atmospheric moisture (Q) and sea surface temperature (SST) modulate the event through latent heat exchange and associated circulation changes. Grid-point mean precipitation rate increases by 31 and 38 μm h-1 per grid point, with warming amplified by 2 and 1 °C at Dome C under a 20% increase in Q and a ~1.3 °C SST increase, respectively. Responses are nonlinear, with AR strength and precipitation more sensitive to reduced Q and enhanced SST. Increased Q accelerates blocking development and AR intensification, promoting an eastward shift of the AR and enhancing precipitation over the ocean. In contrast, SST warming enhances evaporation and moisture retention, producing a delayed but stronger precipitation response. Temperature responses remain uncertain due to cloud radiative effects, highlighting uncertainties in projecting future Antarctic extremes.

DRIVERS OF OBSERVED WINTER–SPRING SEA-ICE AND SNOW THICKNESS AT A COASTAL SITE IN EAST ANTARCTICA

Ricardo Fonseca, Diana Francis; Narendra Nelli; Petra Heil; Jonathan Wille; Irina Gorodetskaya; Robert Massom
Khalifa University, Abu Dhabi, United Arab Emirates

Antarctic sea ice and its snow cover play a pivotal role in regulating the global climate system through feedback on both the atmospheric and the oceanic circulations. Understanding the intricate interplay between atmospheric dynamics, mixed-layer properties, and sea ice is essential for accurate future climate change estimates. This study investigates the mechanisms behind the observed sea-ice and snow characteristics at a coastal site in East Antarctica using in situ measurements in winter–spring 2022. The observed sea-ice thickness peaks at 1.16 m in mid–late October and drops to 0.06 m at the end of November, following the seasonal solar cycle. On the other hand, the snow thickness variability is impacted by atmospheric forcing, with significant contributions from precipitation, Foehn effects, blowing snow, and episodic warm and moist air intrusions, which can lead to changes of up to 0.08 m within a day for a field that is in the range of 0.02–0.18 m during July–November 2022. A high-resolution simulation with the Polar Weather Research and Forecasting model for the 14 July atmospheric river (AR), the only AR that occurred during the study period, reveals the presence of AR rapids and highlights the effects of katabatic winds from the Antarctic Plateau in slowing down the low-latitude air masses as they approach the Antarctic coastline. The resulting convergence of the two airflows, with meridional wind speeds in excess of 45 m/s, leads to precipitation rates above 3 mm/h around coastal Antarctica. The unsteady wind field in response to the passage of a deep low-pressure system with a central pressure that dropped to 931 hPa triggers satellite-derived pack ice drift speeds in excess of 60 km/d and promotes the opening up of a polynya in the Southern Ocean around 64° S, 45° E from 14 to 22 July. Our findings contribute to a better understanding of the complex interactions within the Antarctic climate system, providing valuable insights for climate modeling and future projections.

CONTRASTING RADIATIVE REGIMES IN ANTARCTICA: EMPIRICAL AND ARDL MODELING AND ATTRIBUTION OF GLOBAL SOLAR RADIATION LOSSES AT DOME C AND HORSESHOE ISLAND

Erhan Arslan

Turkey has been conducting regular scientific expeditions to Horseshoe Island in Antarctica since 2017, and the Eighth National Antarctic Scientific Expedition (TAE-VIII) was carried out in 2024. Within the scope of this expedition, meteorological stations were established on Horseshoe Island under project number 122N649, supported by TÜBİTAK (The Scientific and Technological Research Council of Turkey). This study analyzes observational data from Horseshoe Island and Dome C, located in the interior of Antarctica. The characteristics of surface global solar radiation were examined for these two regions with distinct atmospheric and geographical conditions, and atmospheric radiation losses (absorption and scattering) were quantified. In addition, the contributions of these losses to the total radiation budget were compared, relationships between radiation components and meteorological parameters were analyzed, and temporal variations were evaluated. An empirical model based on observations was also developed to estimate global solar radiation, and its performance was tested under two different atmospheric regimes. The analysis covers the period from October 2018 to December 2021 for Dome C and from February 2024 to February 2026 for Horseshoe Island. During these periods, the monthly mean global radiation, water vapor pressure, and temperature were approximately 0.97 MJ/m^2, 0.10 hPa, and −47 °C at Dome C, and 0.60 MJ/m^2, 4.15 hPa, and −1.01 °C at Horseshoe Island, respectively. These results indicate that Horseshoe Island has a significantly more humid atmosphere compared to Dome C. Global radiation was estimated using both empirical formulations and ARDL statistical models based on observed radiation and meteorological parameters. The empirical model showed relatively low performance for Horseshoe Island (R^2 = 0.67), while it performed very well for Dome C (R^2 = 0.99). The ARDL model improved the performance for Horseshoe Island, increasing the R^2 value to 0.89. Overall, radiation losses at Dome C are primarily controlled by molecular absorption and long optical path effects, whereas at Horseshoe Island, scattering processes associated with atmospheric humidity and aerosols play a significant role in shaping the total radiation losses.

A 30-YEAR SATELLITE DERIVED CLIMATOLOGY OF LANDFALLING ANTARCTIC CLOUD MASS MERIDIONAL TRANSPORT EVENTS

Jonathan Chambers[1,2], Matthew Lazzara[1,2,3], Hannah Zanowski[2], David Mikolajczyk[1], Caleb Cullum[1,2], and Mary Reinhardt[1,2]
[1]Antarctic Meteorological Research and Data Center, Space Science and Engineering Center, University of Wisconsin-Madison
[2]Department of Atmospheric and Oceanic Sciences, University of Wisconsin-Madison
[3]Department of Physical Sciences, Madison Area Technical College

1. INTRODUCTION

Antarctica is one of the coldest and driest places on Earth. Orographic lifting along the coastline provides some of this limited precipitation, yet a majority of the heat and moisture is transported from the tropics and mid-latitudes. The latter of these methods is a key contributor to the annual snow accumulation on the ice sheets (Gorodetskaya et al., 2014; Maclennan et al., 2022). The heat and moisture required for precipitation over Antarctica spawns within deep convection events in the tropics (Clem et al., 2022). As these events move poleward, the influx of warm moisture may embed itself into an extratropical cyclone, a polar low, or an atmospheric river (AR). (Hirasawa et al., 2013; Ralph et al., 2017). Should any of these weather systems move poleward over the continent, they are monitored to determine if they are a Cloud Mass Meridional Transport event (CMMT). A CMMT is defined as a landfalling poleward propagating cloud mass over Antarctica for greater than 48 hours. CMMTs are likely a superset of extratropical cyclones and ARs since the overall structure of the cloud mass is irrelevant to their definition.

The Antarctic Meteorological Research and Data Center (AMRDC) used hourly infrared satellite composites from archived data to develop a 30-year climatology for identifying and tracking CMMTs from November 1992-December 2022. This process integrates geostationary and polar-orbiting observations into a single South Pole stereographic projection to combat the limitations of geostationary and polar-orbiting satellites over Antarctica (Kohrs et al., 2013). This climatology is one of the first Antarctic atmospheric climatologies to forgo climate models and reanalyses in favor of satellite imagery. The use of satellites to document the troposphere is not foreign to Antarctica. However, many of these projects were limited to less than five years, or the observations were taken on 3-hourly and monthly intervals (Verlinden et al., 2011; Young et al., 2018).

An objective of this CMMT climatology is to improve operational forecasting capabilities on the continent and to serve as a verification method for numerical based products.

2. METHODS

The goal of tracking CMMTs is to identify long-duration (greater than 48 hours), high-impact, landfalling weather events over Antarctica. Thus, it is expected that a CMMT propagates poleward for its entire duration, can move into Antarctica's interior, its clouds are vertically developed, and it can sustain itself for longer than two days.

The satellite composite images were originally produced in three-hourly intervals before transitioning to hourly intervals in April 2009. Technological advancements have also improved

* Corresponding author address: Jonathan Chambers, University of Wisconsin-Madison, Antarctic Meteorological Research and Data Center, Madison, WI 53706; e-mail: jmchambers3@wisc.edu

the spatial resolution of satellite images, making it easier to identify changes in the speed and direction of the cloud masses.

The climatology is divided into seven regions across the continent: two in West Antarctica and five in East Antarctica (Fig. 1). The Antarctic Peninsula, Ross Ice Shelf, and the Filchner and Ronne Ice Shelves are excluded from this study due to the substantial amount of research already done and the complexity of mesoscale processes in these regions.

The meridional wind component, despite being the dominant wind vector for CMMTs, is coupled to the zonal winds over the Southern Ocean. If an event zonally shifts between two or more regions while continuously satisfying the CMMT criteria, then they are designated as a West or East Antarctic Skirting event.

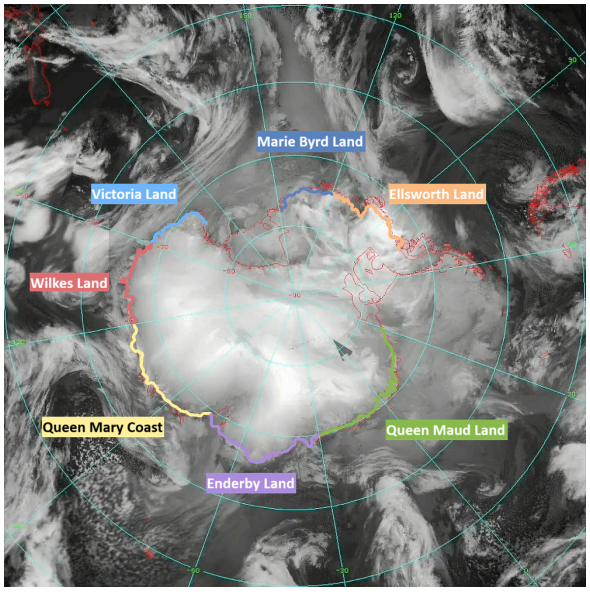

Fig. 1: A satellite composite of the seven regions used in the CMMT climatology. A CMMT is initially tracked when it makes landfall over one of the colored boundaries.

3. RESULTS

The location, duration, seasonality, and the frequency of the CMMTs are analyzed over the entire 30-year time period. A total of 1388 CMMTs were identified, affecting approximately 3907 days. When broken down into five-year periods, CMMTs occurred more often between 1998-2002 and 2008-2012. CMMTs lasted about 2.81 days (or two days and 19 hours) on average. 91% of events ended up between two and four days in duration, but the longest recorded CMMT lasted over 13 days in May 1998.

Around 60% of all CMMTs made landfall in East Antarctica. The busiest individual regions are Ellsworth Land in West Antarctica and Queen Maud Land in East Antarctica at 14% and 13% respectively. However, skirting events were the most common type of CMMT. They made up approximately 49% of the total events. Austral winter (June-August) was the most active season with 390 landfalling CMMTs or approximately 28% of the total events. Conversely, austral summer (December-February) was the least active with 269 or 19% of the CMMTs.

The data collected from this climatology will be used to compare satellite observations to reanalysis forecasting models like ECMWF Reanalysis v5 (ERA5) or the Antarctic Mesoscale Prediction System (AMPS). Diagnostic variables like eddy kinetic energy, moisture flux convergence, and integrated vapor transport can be applied to the reanalysis data to verify the timing and location of the CMMTs.

4. DATA AVAILABILITY

All of the data used are publicly accessible at the Antarctic Meteorological Research and Data Center at the University of Wisconsin-Madison. The satellite composite imagery and animations utilized to track the temporal and spatial distribution of each CMMT can be found at the following link: https://doi.org/10.48567/y8as-0m56 (AMRDC, 2026). The satellite-based 30-year Antarctic landfalling CMMT dataset will be available soon as a comma-separated value file along with monthly ASCII text files detailing the time and location of every CMMT. These files are currently being prepared for public release as of June 2026.

5. ACKNOWLEDGEMENTS

The authors are thankful for the support of the National Science Foundation grants: 1924730, 1951720, 1951603, 2301362. Appreciation must

also be given to the United States Antarctic Program, the Directorate for Geosciences, and the Office of Polar Programs for supporting the AMRDC team both in and out of the field.

6. REFERENCES

Antarctic Meteorological Research and Data Center: Antarctic Satellite Composite Imagery. AMRDC Data Repository. Subset used: [Nov 1992] - [Dec 2022], accessed 05-06-2026, https://doi.org/10.48567/y8as-0m56.

Clem, K. R., D. Bozkurt, D. Kennett, J. C. King, and J. Turner, 2022: Central Tropical Pacific convection drives extreme high temperatures and surface melt on the Larsen C Ice Shelf, Antarctic Peninsula. Nature Communications, 13, doi:10.1038/s41467-022-31119-4.

Gorodetskaya, I. V., M. Tsukernik, K. Claes, M. F. Ralph, W. D. Neff, and N. P. Van Lipzig, 2014: The role of atmospheric rivers in Anomalous snow accumulation in East Antarctica. *Geophysical Research Letters*, **41**, 6199–6206, doi:10.1002/2014gl060881.

Hirasawa, N., H. Nakamura, H. Motoyama, M. Hayashi, and T. Yamanouchi, 2013: The role of synoptic‐scale features and advection in prolonged warming and generation of different forms of precipitation at Dome Fuji Station, Antarctica, following a prominent blocking event. Journal of Geophysical Research: Atmospheres, 118, 6916–6928, doi:10.1002/jgrd.50532.

Kohrs, R. A., M. A. Lazzara, J. O. Robaidek, D. A. Santek, and S. L. Knuth, 2014: Global Satellite Composites — 20 years of evolution. Atmospheric Research, 135–136, 8–34, doi:10.1016/j.atmosres.2013.07.023.

Maclennan, M. L., J. T. Lenaerts, C. Shields, and J. D. Wille, 2022: Contribution of atmospheric rivers to Antarctic precipitation. Geophysical Research Letters, 49, doi:10.1029/2022gl100585.

Ralph, F. M., and Coauthors, 2017: Atmospheric Rivers emerge as a global science and applications focus. Bulletin of the American Meteorological Society, 98, 1969–1973, doi:10.1175/bams-d-16-0262.1.

Verlinden, K. L., D. W. Thompson, and G. L. Stephens, 2011: The three-dimensional distribution of clouds over the Southern Hemisphere high latitudes. Journal of Climate, 24, 5799–5811, doi:10.1175/2011jcli3922.1.

Young, A. H., K. R. Knapp, A. Inamdar, W. Hankins, and W. B. Rossow, 2018: The International Satellite Cloud Climatology Project H-Series Climate Data Record Product. Earth System Science Data, 10, 583–593, doi:10.5194/essd-10-583-2018.

HEATWAVES IN THE EAST ANTARCTIC INTERIOR AMPLIFIED BY CLIMATE CHANGE

Naoyuki Kurita, David H. Bromwich, Matthew A. Lazzara
Nagoya University

Recognition of a warming trend in the Antarctic Peninsula and West Antarctica since the mid-20th century has prompted significant growth in research. By contrast, research on climate change in East Antarctica (EA) has been far less extensive, with the region being considered less sensitive to ongoing climate change. However, recent studies have cast doubt on this view. The interior of EA has experienced warming and an increase in temperature extremes. Notably, the most pronounced warming has occurred in the eastern Dronning Maud Land (DML) from spring to summer since the early 1990s. Here, we explore the physical mechanisms responsible for these changes using observational data from the eastern DML between 1994 and 2024. We also investigate whether these changes are caused by natural variability or are the result of anthropogenic warming.

Temperature records from three inland stations (Mizuho, Relay Station, and Dome Fuji) showed that the frequency of daily mean temperatures has shifted towards warmer conditions. There has been an increase (decrease) in the frequency of extremely warm (cold) days at Dome Fuji and Relay Station over the past 30 years. This increase in temperature extremes has notably contributed to the regional warming trend during the warm season (October to February), resulting in a rapid warming that is more than twice as fast as the global mean.

These temperature extremes did not manifest as brief heat spikes, but rather as heatwaves lasting several days. These extreme events were triggered by the heat transport via a blocking high-pressure ridge that developed from the southern Indian Ocean (IO) into the interior of EA. The occurrence of the blocking ridges over the southern IO is closely linked to the strength of the westerly winds. Since the late 2000s, mid-latitude westerly winds in the southern IO have weakened, making the blocking patterns more likely to occur. The increased occurrence of the blocking ridges in recent years has led to higher seasonal mean temperatures and an increased frequency of temperature extremes in the eastern DML. However, the recent change in the atmospheric circulation can account for only half of the observed temperature changes that have occurred over the past 30 years. Therefore, the remaining temperature increase must be attributed to a thermodynamic driver, such as the enhanced heat transport associated with the blocking ridge.

How much do extreme snowfall events contribute to the mass of the Antarctic Ice Sheet?

Karissa Shannon[1], Tristan L'Ecuyer[1], Marian Mateling[1]
[1]University of Wisconsin–Madison

1 Introduction

The Antarctic Ice Sheet (AIS) plays a critical role in global sea level regulation in a warming climate. Snowfall is a key factor in ice mass balance, influencing the ice sheet's contribution to sea level changes. Previous studies have shown that moisture intrusions can cause large snowfall events, but by focusing only on the most extreme moisture events impinging on the ice sheet, these studies only address specific regions of the ice sheet, omitting many potential mass-building snowfall events across other parts of the continent. This study examines extreme snowfall events across drainage basins and elevation bands using the new Combined CloudSat CALIPSO Snowfall (C3S).

2 Data and Methods

Snowfall rates are obtained from the CloudSat and CALIPSO Combined Snow (C3S) product, which combines CloudSat radar retrievals with CALIPSO lidar observations to improve snowfall estimates near the surface. The analysis focuses on the 2007–2010 period, when CloudSat provided the most complete day-night sampling. Extreme snowfall is defined as snowfall rates exceeding the 95th percentile snowfall rate for a given region. The contribution of extreme snowfall to total accumulation is calculated as the fraction of annual accumulation associated with snowfall rates above this threshold. We also determine the snowfall rate responsible for half of the annual accumulation and its corresponding percentile within the snowfall-rate distribution. To understand the spatial variability in the role of extreme events across the AIS, we divide the AIS in two ways: elevation bands and drainage basins. Previous studies have shown that snowfall accumulation varies significantly with elevation, with higher elevations typically receiving less accumulation than coastal areas (Palerme et al. [2014]). Here, we define seven elevation categories, each covering a 600-meter range, from 0 - 0.6 km through 3.6 - 4.2 km. This division allows us to characterize variations in extreme snowfall contributions across elevation bands. However, this elevation perspective is not ideally-suited to mass budget studies since the relative importance of ablation processes can vary significantly within any given elevation band and blowing snow systematically transports snow across elevation bands. We therefore also analyze extreme snowfall across drainage basins. Drainage basins are defined by Zwally et al. [2012], which reflect consistent surface slope relative to atmospheric advection and ice mass balance can be considered independently for each.

3 Results

The C3S dataset indicates that snowfall contributed approximately 1400 Gt yr^{-1} of mass to the Antarctic Ice Sheet during 2007–2010. The 95th percentile snowfall rate is 0.57 mm hr^{-1} for the whole continent. We find that the top 5% most intense snowfall events account for 40.3% of the total annual accumulation over the ice sheet. In addition, the snowfall rate responsible for half of the annual accumulation is 0.42 mm hr^{-1}, corresponding to the 92.5th percentile of snowfall rates. In other words, the top 7.5% most intense snowfall events contribute half of the annual Antarctic snowfall accumulation. Substantial regional variability is evident when the analysis is repeated by elevation band. Snowfall mass and frequency decrease with increasing elevation, while the threshold for extreme snowfall declines by more than an order of magnitude, from approximately 0.8 mm hr^{-1} in coastal regions to 0.05 mm hr^{-1} in the highest elevation band. Despite this large change in snowfall intensity, the fraction of accumulation associated with extreme snowfall remains relatively consistent through most of the ice sheet, ranging from approximately 34–37% below 3 km elevation. In contrast, extreme snowfall becomes substantially less important in the highest elevations of Antarctica. Above 3.6 km elevation, only 19.5% of total accumulation is associated with snowfall rates exceeding the local 95th percentile threshold. Similarly, more than one-quarter of snowfall events are required to account for half of the total accumulation in the highest elevation band, compared to only 9–12% of snowfall events in lower-elevation regions. These results indicate that snowfall-rate distributions become less skewed at the highest elevations, reducing the relative importance of extreme events for total accumulation. An additional analysis performed across Antarctic drainage basins reveals regional variability in the contribution of extreme snowfall events. More coastal basins characterized by frequent cyclonic activity exhibit the largest contributions from extreme snowfall, with more than one-third of total accumulation associated

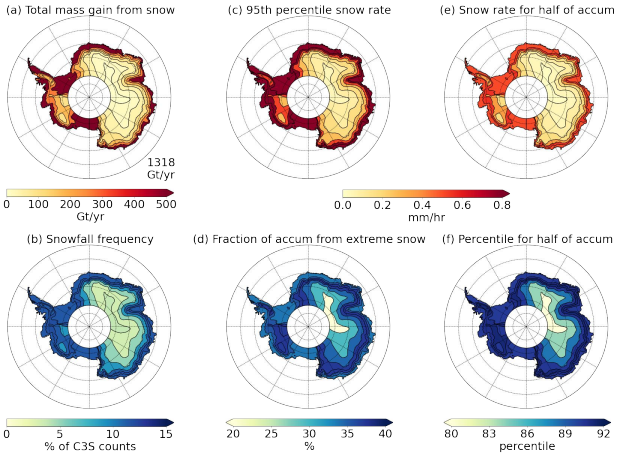

Figure 1: (a) The total mass gain from snowfall and (b) snowfall frequency for different elevation bands on the Antarctic Ice Sheet between 2007 - 2010. (c) shows the 95th percentile snowfall rate and (d) the fraction of accumulation from extreme snowfall for this period while (e) and (f) show the threshold snowfall rate and which accounts for half of the accumulation and its percentile within the full snowfall rate PDF for each elevation band.

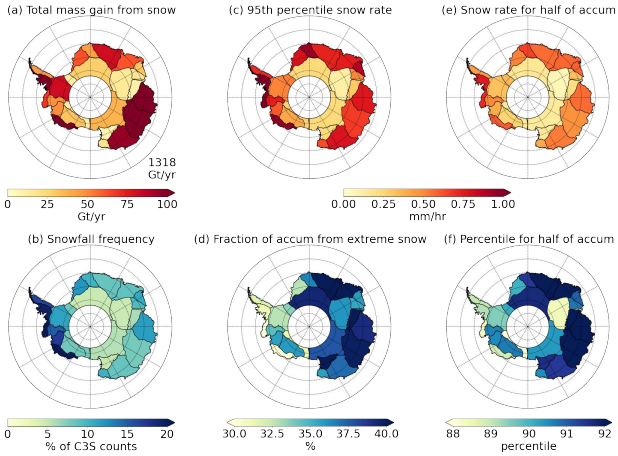

Figure 2: As in Figure 1. but for the drainage basins defined by Zwally et al. [2012].

with events exceeding the local 95th percentile threshold. In contrast, interior basins show a weaker dependence on extreme events, consistent with the elevation-based analysis. Despite these regional differences, extreme snowfall remains an important contributor to Antarctic mass input across nearly all basins, highlighting the role of extreme snowfall in shaping the annual snowfall accumulation.

4 Conclusions

Extreme snowfall events play a critical role in Antarctic accumulation. Across the continent, the top 5% of snowfall events contribute approximately 40% of total snowfall accumulation, while the top 7.5% of events contribute half of the annual accumulation. However, the importance of extreme snowfall varies considerably across the ice sheet. Coastal and lower-elevation regions rely more heavily on intense snowfall events for mass gain, whereas accumulation in the highest portions of the Antarctic interior is derived from a broader range of snowfall intensities. These findings highlight the importance of understanding how future changes in atmospheric moisture transport and storm activity may influence Antarctic snowfall and ice-sheet mass balance.

References

C. Palerme, J. E. Kay, C. Genthon, T. L'Ecuyer, N. B. Wood, and C. Claud. How much snow falls on the Antarctic ice sheet? *The Cryosphere*, 8(4):1577–1587, August 2014. ISSN 1994-0416. doi: 10.5194/tc-8-1577-2014. Publisher: Copernicus GmbH.

H. Jay Zwally, Mario B. Giovinetto, Matthew A. Beckley, and Jack L. Saba. Antarctic and Greenland Drainage Systems. *GSFC Cryospheric Sciences Laboratory*, 2012.

REVISITING THE EXTRAORDINARY KATABATIC WIND REGIME AT TERRA NOVA BAY, ANTARCTICA

Brian Rakoczy, David Bromwich
The Ohio State University

Terra Nova Bay, Antarctica, contains one of the most intense katabatic wind confluence zones on the continent, where drainage from the East Antarctic plateau accelerates through glacier valleys before exiting into the western Ross Sea. Using quality-controlled observations from automatic weather stations and staffed stations spanning 1995–2025, an updated climatology of the Terra Nova Bay wind regime was developed to examine the spatial structure, seasonality, and persistence of high-wind events. Particular focus is placed on observations from the Manuela automatic weather station on Inexpressible Island, where installation of an updated high-wind anemometer in 2012 has provided an improved continuous record within the core outflow region. Results show strong acceleration along the drainage pathways, with mean winter wind speeds exceeding 20 m s^{-1} near the coastal outlet. More than 1000 prolonged severe and extreme wind events were identified, including events continuously lasting to 14 days. Preliminary analysis suggests that the longest events occur when katabatic and synoptic scale forcing are aligned.

A November Snow Event at McMurdo Station

John R Michael
Chickasaw Alliance Group/NIWC Office of Polar Programs

On November 18, 2024, snow struck Williams Field, on the Ross Ice Shelf near McMurdo Station. Observer-reported visibility fell to less than one mile - unfortunately below safe thresholds for two aircraft due to land at the field at that time. Fortunately, visibility remained high enough for successful landings accomplished at nearby Phoenix Field.

Examination of the available satellite imagery, surface observations, and AMPS graphic model output for that day illustrates the physical limitations of currently available weather observing and forecasting systems at these critical airfields, and indicates the enhancements to safe flying operations to be gained by adding weather radar to that inventory. Imagery from the 2019 deployment of a Doppler radar system to Phoenix Airfield near McMurdo Station suggests not just the critical improvements to short-term forecasting offered by a permanent installation, but also abundant avenues for future cooperative efforts of mutual benefit to the research and operational Antarctic meteorological communities in the years ahead.

The November 2024 Snow Event

Model output from AMPS has become an indispensable tool for forecasters in the Unted States Antarctic Program. In a recent example, graphic products generated during an unprecedented wintertime cross-continental aircraft mission revealed a window of opportunity for a flight from McMurdo to South Pole to Rothera days before the successful attempt. AMPS has repeatedly proven reliable in this regard. November 18, 2024, is a rare exception. An unanticipated snow event reduced visibility at Williams Field to below the safe landing minimum, resulting in aircraft diversions to Phoenix Field. Satellite imagery offers an excellent big-picture/top-down overview of the event, but in addition to only *inferring* surface conditions is generally not available to forecasters in real-time, and often not until one half to one hour (or more) after capture.

The challenge

The dilemma a forecaster faces in this circumstance is what information can be given a pilot to assist in weighing alternatives to determine the safest available options in a time-critical situation. The November 2024 event is a more dramatic example than typical. However, while rare, the overall situation is inevitable given the relatively large number of missions flown to or from McMurdo's airfields during an Antarctic operational season. Key examples would include point of safe return (PSR) forecasts delivered to pilots flying Christchurch to McMurdo missions, especially those during which some other unforeseen weather event has occurred at their destination. The cost of wrong decisions made at this point can be measured in dollars and lives.

The November 2019 Snow Event

NPP facilitated a temporary Doppler radar installation at Phoenix Airfield during the 2019 operational season. Data captured is available as compressed jpg images at AMRDC. The author has generated several animations of these files, initially captured on 13 and 14 November that year. The first day of this event was characterized by light snow, with visibility remaining unrestricted throughout. The second saw heavier snowfall, with minimum reported visibility at the airfield at or below 800 meters. The first day's radar output offers a clear indicator to a forecaster that unrestricted visibility – thus safe flying conditions - was likely to persist; the second that it would not. However, once the visibility had fallen, confidence in timing of a forecast improvement would likewise be greatly enhanced.

Conclusion

The applicability of the radar observations to the challenge described is clear to those familiar with the operating environment, but as of now observational and anecdotal only. Additional avenues for research using Doppler radar data will be abundant once a permanent installation is in place. Beneficiaries of this research would include the crew and passengers of the aircraft involved, and any others with an interest in minimizing resource expenditure while maximizing the effective use of limited time available for conducting research and operations in the Antarctic environment.

USE OF TALL TOWER DATA IN OPERATIONAL FORECASTING

Bella Onsi
NIWC LANT Polar Programs

One of NPP weather's primary responsibilities is providing aviation forecasts and briefings to crews flying in and out of the USAP airfields. In addition to satellite imagery and model data, forecasters utilize surface observations from the AWS Network around McMurdo Station and the flight destination when creating their forecasts. However, these AWS only provide observations near the surface. The Tall Towers provide forecasters and scientists with weather measurements from multiple points from the surface up to 30m above the surface, giving a more robust depiction of what is happening in that column of air. This presentation will highlight the benefits of having access to weather observations from Tall Towers (specifically Elijah Tall Tower) for operational forecasting as well as plans for future uses for the data.


NSF
UNITED STATES ANTARCTIC PROGRAM
NATIONAL SCIENCE FOUNDATION